PB81-172256

Optimum Meteorological and Air Pollution Sampling Network Selection in Cities
Volume III: Objective Variational Analysis Model

Research Triangle Inst.
Research Triangle Park, NC

Prepared for

Environmental Monitoring and Support Lab.
Las Vegas, NV

Mar 81

U.S. Department of Commerce
National Technical Information Service
NTIS.

TECHNICAL REPORT DATA
(Please read Instructions on the reverse before completing)

1. REPORT NO.	2.	3. RECIPIENT'S ACCESSION NO.
EPA-600/4-81-012	ORD Report	PB81 172256

4. TITLE AND SUBTITLE	5. REPORT DATE
OPTIMUM METEOROLOGICAL AND AIR POLLUTION SAMPLING NETWORK SELECTION IN CITIES. Volume III: Objective Variational Analysis Model	March 1981
	6. PERFORMING ORGANIZATION CODE
7. AUTHOR(S)	8. PERFORMING ORGANIZATION REPORT NO.
W. D. Bach, Jr., and F. M. Vukovich	
9. PERFORMING ORGANIZATION NAME AND ADDRESS	10. PROGRAM ELEMENT NO.
Research Triangle Institute P.O. Box 12194 Research Triangle Park North Carolina 27707	11. CONTRACT/GRANT NO. 68-03-2187
12. SPONSORING AGENCY NAME AND ADDRESS	13. TYPE OF REPORT AND PERIOD COVERED
U.S. Environmental Protection Agency--Las Vegas, NV Office of Research and Development Environmental Monitoring Systems Laboratory Las Vegas, NV 89114	14. SPONSORING AGENCY CODE EPA/600/07

15. SUPPLEMENTARY NOTES

J. L. McElroy, EMSL-LV, Project Officer

16. ABSTRACT

This report is the third in a series of reports on the development and application of a procedure to establish an optimum sampling network for ambient air quality in urban areas. In the first report, the theoretical aspects and the model algorithms for the procedure and an optimum network for St. Louis were presented (EPA-600/4-78-030). The results of the comparison of the wind field obtained from the optimum network in St. Louis and that obtained from all available data were described in the second report (EPA-600/4-79-069). This report discusses the development and application to St. Louis of the Objective Variational Analysis Model which is used to provide the air pollution distribution.

17. KEY WORDS AND DOCUMENT ANALYSIS

a. DESCRIPTORS	b. IDENTIFIERS/OPEN ENDED TERMS	c. COSATI Field/Group
Meteorology Air pollution	Objective Variational Analysis St. Louis, MO. Model algorithms	55C 68A

18. DISTRIBUTION STATEMENT	19. SECURITY CLASS (This Report)	21. NO. OF PAGES
RELEASE TO PUBLIC	UNCLASSIFIED	69
	20. SECURITY CLASS (This page)	22. PRICE
	UNCLASSIFIED	

PB81-172258

BEGIN FIRST LINE OF TEXT HERE
TYPING GUIDE SHEET
CENTER OF PAGE
TOP OF IMAGE AREA
DROPPED HEAD; BEGIN SECTIONS HERE

EPA 600/4-81-012
March 1981

OPTIMUM METEOROLOGICAL AND AIR POLLUTION SAMPLING NETWORK SELECTION IN CITIES

Volume III: Objective Variational Analysis Model

by

Walter D. Bach, Jr. and Fred M. Vukovich
Research Triangle Institute
P.O. Box 12194
Research Triangle Park
North Carolina 27707

Contract No. 68-03-2187

Project Officer
James L. McElroy
Advanced Monitoring Systems Division
Environmental Monitoring System Laboratory
Las Vegas, Nevada 89114

ENVIRONMENTAL MONITORING SYSTEMS LABORATORY
OFFICE OF RESEARCH AND DEVELOPMENT
U.S. ENVIRONMENTAL PROTECTION AGENCY
LAS VEGAS, NEVADA 89114

BEGIN LAST LINE OF TEXT
BOTTOM OF IMAGE AREA OUTSIDE DIMENSION FOR TABLES AND ILLUSTRATIONS
3/8"
PAGE NUMBER
EPA-287 (Cin.)
(4-76)

PRODUCT OF:
NATIONAL TECHNICAL INFORMATION SERVICE
U.S. DEPARTMENT OF COMMERCE
SPRINGFIELD, VA. 22161

BEGIN FIRST LINE OF TEXT HERE
TYPING GUIDE SHEET
CENTER OF PAGE
TOP OF IMAGE AREA
DROPPED HEAD, BEGIN SECTIONS HERE
6-1/2"
9-1/8"
BEGIN LAST LINE OF TEXT
3/8"
BOTTOM OF IMAGE AREA, OUTSIDE DIMENSION FOR TABLES AND ILLUSTRATIONS
PAGE NUMBER
EPA-287 (Cin.)
(4-76)

DISCLAIMER

This report has been reviewed by the Environmental Monitoring Systems Laboratory, U.S. Environmental Protection Agency, and approved for publication. Approval does not signify that the contents necessarily reflect the views and policies of the U.S. Environmental Protection Agency, nor does mention of trade names or commercial products constitute endorsement or recommendation for use.

BEGIN FIRST LINE OF TEXT HERE
TYPING GUIDE SHEET
CENTER OF PAGE
TOP OF IMAGE AREA
DROPPED HEAD; BEGIN SECTIONS HERE

SUMMARY

This report is the third in a series treating a method for developing optimum meteorological and air quality networks and the application of the methodology for St. Louis. (EPA-600/4-78-030 describes the method and the network for St. Louis and EPA-600/4-79-069 presents an evaluation of the meteorological (wind field) network for St. Louis.) This particular report discusses the development and application to St. Louis of the Objective Variational Analysis Model (OVAM), which is used to provide estimates of the air pollution distribution.

The OVAM produces an analysis of air quality in an area by solving an Euler-Lagrange equation that minimizes the weighted error variance between the analysis and observations and between the analysis and the solution from the equation of mass continuity. The OVAM was applied to obtain analyses of carbon monoxide, CO, in the St. Louis area for selected days in August, 1975 and February, 1976, periods of intensive study by the Regional Air Pollution Study. Measurements of CO concentration and winds at a 19-station optimum sampling network and the emission inventory were used by the OVAM to estimate the concentrations in a 20-km square area centered on the city. Four cases, totalling 26 hours, were selected for detailed study.

Methodologies to incorporate point sources were developed. Studies of the sensitivity of the analyses to various user-defined parameters showed that the relative weights given to the observations and to the constraint equation were the most important factors. The analytical results became smoother as the depth of the volume increased. The model was insensitive to changes in the radius of influence of an observation.

The OVAM analyses appeared more consistent with the distribution of sources and winds than were found using conventional objective analyses, particularly when emissions were large and consistent with the observations. Plumes of high concentration appeared downwind of the major sources, except when observations indicated otherwise. In areas of low emissions, the OVAM did not change the results significantly. The error variance throughout the area of analysis decreased by about 25 percent from its initial value. At night, the emissions were small compared to the observations and were insufficient to alter the initial estimate of the distribution. For these situations, the effects of adjustments to boundary conditions and advection predominated.

BEGIN LAST LINE OF TEXT
BOTTOM OF IMAGE AREA; OUTSIDE DIMENSION FOR TABLES AND ILLUSTRATIONS
3/8"

EPA-287 (Cin.)
(4-76)

The OVAM generally predicted the trends well but often failed to accurately predict the absolute magnitudes of CO concentrations at nonnetwork stations. In addition to model errors, the discrepancies arose because:

1. CO concentrations are often very source-oriented and sources were smoothed to a 1-km square area by the inventory (the problem affects all CO data), whereas the observations are point observations not necessarily representative of an area, and

2. OVAM values used for comparisons were at grid points up to 0.7 km from an observation, and plumes downwind of principal sources developed with strong gradients which may have a slight influence at the grid point which actually affects the station, or vice-versa.

These are shortcomings faced by modelers and analysts every day.

The consequences of randomly deleting two, four or six observations from the analyses were investigated to develop guidance as to which, if any, of the observations could be deleted from the analysis, without significantly affecting the analysis. This was done to determine if all the stations in the optimum network needed to monitor CO. The analyses showed the average error variance reduction did not change, although large percentage changes were noted in localized sections of the analyses. Some changes were due to changes in the initial analysis; other changes (usually increases) were due to the dominance of the mass continuity equation, where observations, which had been removed, had previously dominated.

When stations were deleted in regions with small or no emissions (the outlying regions of the city) and far from stations influenced by large sources, the impact was significant in those regions but relatively insignificant in the large emissions' areas. The impact of the deleted stations in the outlying region was primarily due to the initial values being different from the observations, suggesting that if initial conditions can be treated properly in the outlying regions, some of the stations in this region would not be required as CO monitors. Thirteen of the 19 stations were in such regions; possibly as many as half of these need not monitor CO, though they all must monitor the winds. However, further investigation is required on the initialization methodology before conclusive statements can be made.

Though the optimization technique has been used to develop an entire network, probably its greatest practical utility can be in improving an existing network in a given urban area. Most urban areas already have a sampling network and would not want to undertake the economic burden to establish a new network.

BEGIN FIRST LINE OF TEXT HERE
TYPING GUIDE SHEET
mk-41-80
CENTER OF PAGE
TOP OF IMAGE AREA
DROPPED HEAD, BEGIN SECTIONS HERE

CONTENTS

	Page
Summary	iii
Figures	vi
Tables	vii
Introduction	1
Background	1
Objective variational analysis model	4
Research objectives	5
Model Development	7
Model equations	7
Study area	11
Point sources	11
Profile parameter	11
Aerometric data	14
Objective analysis	14
Relaxation procedure	14
Options	15
Model Applications	18
Selection of cases	18
Model performance	18
Model sensitivity	26
Time sequence of analyses: 12 August 1975	27
Deletion of observations	36
Effects of boundary conditions on analyses	47
Error variance	51
Accuracy estimates	51
Discussion of Results	54
Major findings	54
Limitations and further research	55
Utilization of the OSN technique	57
References	58
Appendix A	60

BOTTOM OF IMAGE AREA, OUTSIDE DIMENSION FOR TABLES AND ILLUSTRATIONS
BEGIN LAST LINE OF TEXT HERE
3/8"

PAGE NUMBER
EPA-287 (Cin.)
(4-76)

BEGIN FIRST LINE OF TEXT HERE
TYPING GUIDE SHEET
CENTER OF PAGE
TOP OF IMAGE AREA
DROPPED HEAD; BEGIN SECTIONS HERE

FIGURES

Number		Page
1	Location of stations in the RTI network and other non-network stations used in the evaluation in the St. Louis metropolitan area.	3
2	OSN network and OVAM analysis area	12
3	Response of OVAM analysis to point source plume rise above and below the top of the model, Z.	13
4	Ratio of weights, $\tilde{\alpha}/\alpha$, as a function of ALFA and RAD	17
5	Hourly CO concentrations at OSN locations.	19
6	Wind vectors, area sources, and CO isopleths, August 12, 1975 at 1300 CST	25
7	Isopleths of CO concentration for basic state of sensitivity analyses and isopleths of percent change from basic state induced by indicated parameter value	28
8	Spatial cross section of OVAM analysis for sensitivity tests indicated in key	30
9	OVAM concentration analyses and area emissions by hour for August 12, 1975.	32
10	Time series of observed and interpolated CO concentrations for indicated number of missing observations for August 12	39
11	Isopleths of concentration for basic case and percent change with two, four or six stations deleted, August 12, 1975.	41
12	Isopleths of concentration for basic case and percent change with two, four, or six stations deleted, February 27, 1976.	48
13	Time series of CO concentrations for OSN and non-OSN locations from observations, Barnes interpolation and OVAM analysis with zero or six stations missing	50

BEGIN LAST LINE OF TEXT
BOTTOM OF IMAGE AREA; OUTSIDE DIMENSION FOR TABLES AND ILLUSTRATIONS
3/8"

EPA-287 (Cin.)
(4-76)

BEGIN FIRST LINE OF TEXT HERE
TYPING GUIDE SHEET
CENTER OF PAGE
TOP OF IMAGE AREA
DROPPED HEAD; BEGIN SECTIONS HERE

TABLES

Number		Page
1	Parameters of Sensitivity Analysis.	27
2	CO Concentrations Observed and Interpolated by the Barnes and OVAM for OSN Stations Within the Analysis Grid.	37
3	Missing and Deleted Observations, August 12, 1975	38
4	Non-Dimensional Error Variance of Analyses.	52

8-1/2"
9-1/8"
BEGIN LAST LINE OF TEXT
BOTTOM OF IMAGE AREA; OUTSIDE DIMENSION FOR TABLES AND ILLUSTRATIONS
3/8"

PAGE NUMBER
EPA-287 (Cin.)
(4-76)

BEGIN FIRST LINE OF TEXT HERE
TYPING GUIDE SHEET
CENTER OF PAGE
TOP OF IMAGE AREA
DROPPED HEAD: BEGIN SECTIONS HERE

INTRODUCTION

BACKGROUND

The Research Triangle Institute (RTI) has been engaged in a long-term program with the United States Environmental Protection Agency (EPA) to develop and test a methodology to determine an optimum sampling network (OSN) for a major urban area. The research has been motivated by the realization that the costs of implementing a sampling network within budgetary constraints of a control agency may result in fewer stations than desirable but that the stations must be adequate for the task in the present and the future.

Conventional networks are often designed to monitor specific sources or concentration characteristics of a large subsection of the urban area. With different source distributions for different pollutants, a good site for one pollutant may not be good for another. As sources are added or deleted, the monitoring requirements change. As stations are moved, valuable time histories of pollutants are lost.

RTI has taken the approach, contrary to conventional applications, that knowledge of the wind distributions about the urban area should give principal guidance to the design of a network of air quality monitors. The distribution of pollutants is controlled primarily by their sources and by the wind speed and direction. Sources and source distributions change as the urban area changes, but the wind characteristics are not a function of source and should remain relatively unaffected by source changes. Thus, by having a sampling network that will accurately depict the distribution of winds about the urban area, the distribution of pollutants should follow from a knowledge of the source distribution.

The RTI approach involves six steps. Though in the initial case, the technique was employed in St. Louis, Missouri, the algorithms are generalized and can be applied to any urban region. The six steps are:

(1) A three-dimensional hydrodynamic model was developed to generate simulated wind fields for the urban area under a variety of initial meteorological conditions for the St. Louis urban area.

(2) A statistical model was chosen from a class of statistical model forms, relating winds to the geographic location and topography and giving a reasonable approximation to the simulated results for any of the initial conditions.

BEGIN LAST LINE OF TEXT
BOTTOM OF IMAGE AREA, OUTSIDE DIMENSION FOR TABLES AND ILLUSTRATIONS
3/8"

EPA-287 (Cin.)
(4-76)

BEGIN FIRST LINE OF TEXT HERE
TYPING GUIDE SHEET
CENTER OF PAGE
TOP OF IMAGE AREA
DROPPED HEAD; BEGIN SECTIONS HERE

(3) A site selection methodology was developed, and an optimum set of sites for monitoring winds was selected using the methodology and the statistical model.

(4) Wind and air quality monitoring stations were established at the indicated sites in St. Louis.

(5) Wind fields were created by fitting statistical models based on the class of forms determined in Step 2 to the observed data, and the predicted data were compared to observed data.

(6) An objective variational model was developed and tested to estimate pollution concentrations over the area by combining the emissions inventory, the observed pollutant concentration, and the estimated wind fields.

With minor modifications resulting from practical and economic constraints, the first four steps above were completed for the St. Louis area as described in Volume I (Vukovich, Bach, and Clayton, 1978, hereafter referred to as VBC). Analysis of the wind field obtained from the OSN (Step 5) was described in Volume II (Vukovich and Clayton, 1979). This volume provides the description of the development of the objective variational analysis model, its application, and the results obtained.

The three-dimensional primitive equation model was used to create the wind field in the St. Louis area over a variety of meteorological conditions. These data were used to develop a statistical model to characterize the wind field. The statistical model was combined with a backward elimination site selection technique to produce the OSN. From an initial field of over 500 candidate sites, the resulting OSN had 19 stations.

The major emphasis of the second phase of the research project involved the preparation and execution of a summer and winter field program in St. Louis. These field programs were held during August 1975, and February and March, 1976 when EPA was performing intensive studies of the Regional Air Pollution Study (RAPS). During this time there was a concerted effort to maintain a high level of performance of the twenty-four RAPS surface monitoring stations.

Sixteen existing stations in St. Louis were situated near the OSN station locations, and were used as part of the OSN. Four of the existing stations were St. Louis city/county air pollution stations and twelve were RAPS stations. RTI set up three temporary stations specifically for this research. The stations comprising the OSN network and the non-network in the St. Louis area are shown in Figure 1.

Following the field program, processed network and non-network wind data were used to evaluate the wind field determined from the optimum network. The principal result of that study showed that application of the stepwise regression to a 13-term model (the chosen statistical model) with the wind data from the 19-station OSN predicted wind fields comparable to those obtained by more general procedures, using more terms and a larger network.

BEGIN LAST LINE OF TEXT
BOTTOM OF IMAGE AREA; OUTSIDE DIMENSION FOR TABLES AND ILLUSTRATIONS
3/8"

EPA-287 (Cin.)
(4-76)

BEGIN FIRST LINE OF TEXT HERE
TYPING GUIDE SHEET
CENTER OF PAGE
TOP OF IMAGE AREA
DROPPED HEAD BEGIN SECTION HERE

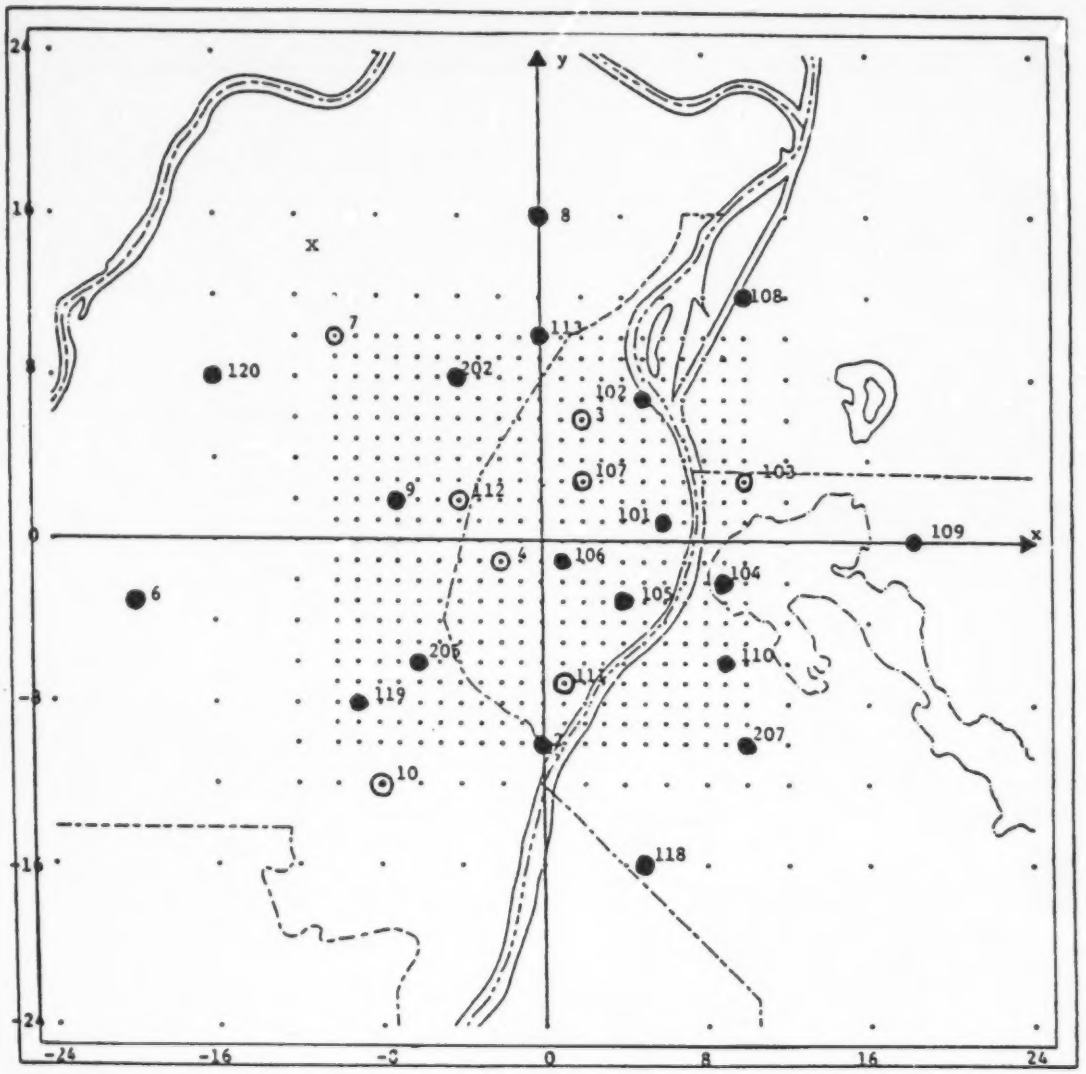

Figure 1. Location of stations in the RTI network (solid dots) and other non-network stations (open dots) used in the evaluation (interior grid spacing = 1 km) in the St. Louis metropolitan area. Lambert Field is shown by x.

BEGIN LAST LINE OF TEXT
3/8"
BOTTOM OF IMAGE AREA, OUTSIDE DIMENSION FOR TABLES AND ILLUSTRATIONS

PAGE NUMBER
EPA-237 (Cin.)
(4-76)

BEGIN FIRST LINE OF TEXT HERE
TYPING GUIDE SHEET
CENTER OF PAGE
TOP OF IMAGE AREA

This substantiated the results of the theoretical analysis which selected the 13-term model and the 19-station OSN on the basis that adding terms to the model and/or stations to the network would not markedly improve the analysis of the wind field.

DROPPED HEAD, BEGIN SECTIONS HERE

OBJECTIVE VARIATIONAL ANALYSIS MODEL

Within an urban area, the pattern of pollutant concentrations is not generally apparent from a set of concentration measurements at fixed locations. The presence of more sources than sampling stations and the variability in the wind field often mask the true distribution from those obtained by conventonal subjective or objective analysis. In conventional objective analysis, the estimated value of a variable at a given location is extrapolated/interpolated from observed values of the variable at specified locations. Cressman (1959) and Barnes (1964) used different distance-dependent weight functions to interpolate within a given radius of an observation. Endlich and Mancuso (1968) used an elliptical weight function oriented along the wind direction and proportional to the wind speed. These techniques smooth the distributions and are generally incapable of showing maxima or minima where there are no observations.

Sasaki (1958, 1970a, b, c) proposed an analysis technique that uses the observed variables to produce analysis which is consistent with both the observations and the model. The technique is based on minimizing the weighted error variance of 1) the arbitrary variable, ϕ , and its observation, $\tilde{\phi}$, and 2) the model equations, $E(\phi)$, over the domain of the integration. The total weighted error variance, EV, is given by:

$$EV = \int_{\Omega} \tilde{\alpha}(\phi-\tilde{\phi})^2 + \alpha E^2(\phi) \quad d\Omega.$$

The terms $\tilde{\alpha}$ and α are the weighting functions and are inversely proportional to the typical variance of their respective terms. This formulation is called the "weak constraint" by Sasaki since $E^2(\phi)$ is being minimized rather than $E(\phi)$. The distinction is significant since $E(\phi)$ is normally zero.

The distribution of ϕ which minimized the intergral is given by the solution to the Euler-Lagrange equations (Lanczos, 1970). The equations specify the partial differential equation of ϕ which must be satisfied on the interior of the domain and the boundary conditions. The solution is generally obtained by numerical integration.

Sasaki and Lewis (1970) used the technique to analyze three-dimensional mesoscale distributions of wind components, temperature, and moisture associated with severe storms. Stephens (1970) obtained synoptic scale distributions of pressure height fields consistent with the balance equation. In those studies, the solution technique acted as a low-pass filter for real or induced (simulated) errors in the observation field.

Wilkins (1971, 1972) applying the objective variational analysis principles to urban air pollution analyses, described a method of adjusting a

BEGIN LAST LINE OF TEXT
BOTTOM OF IMAGE AREA, OUTSIDE DIMENSION FOR TABLES AND ILLUSTRATIONS
3/8"

PAGE NUMBER
EPA-287 (Cin.) (4-76)

BEGIN FIRST LINE OF TEXT HERE
TYPING GUIDE SHEET
CENTER OF PAGE
TOP OF IMAGE AREA
DROPPED HEAD; BEGIN SECTIONS HERE

pattern of concentration isopleths using the classical diffusion equation as a constraint. The technique reduced discrepancies in temporal continuity between two successive analyses. Errors arising from misanalysis or from a variable wind field were also considered. Wilkins showed that the analysis error of the sequences of an analysis could be reduced to one-tenth the initial error. He also outlined the potential application of the methodology as a part of the continuous urban air monitoring surveillance program.

The approach used in this research project reverts to more basic forms. The differential form of the mass continuity equation for a trace material instead of an integrated form is used as a constraint, and the observed concentrations are used where and when they are available. Wilkins' approach could be used to adjust the resulting analyses.

The purpose of an objective analysis is to obtain an estimate of the concentrations where observations are missing. The variational analysis approach requires that the analysis fit the observed concentrations and the emissions, transport, and diffusion characteristics throughout the urban area. The "best analysis" is defined as the distribution which minimizes the weighted sum of the error variance a) between the observed and analyzed concentrations, and b) the departure of the results from a steady state.

In VBC, the essential elements of the objective variational analysis model (OVAM) were developed and explored through idealized cases and a sensitivity analysis. In the case studies, the OVAM developed a solution very similar to an analytic solution even when only a few "observations" were known. When a random error was added to those observations, the OVAM still produced an analysis in close agreement with the analytic solution. The error variance of the initial analysis was reduced by an order of magnitude. The ratio of weights, $\tilde{\alpha}/\alpha$, for the analyses and the boundary conditions had the greatest impact upon the characteristics of the solution obtained.

RESEARCH OBJECTIVES

The primary purpose of this research project was to produce an OVAM that gives better analysis of inert pollutants than conventional objective analysis techniques. In order to accomplish this objective, the following tasks were undertaken:

- The OVAM algorithm was modified to incorporate temporal variability of the air pollutant and to include a more rapidly convergent relaxation technique.
- The results of the OVAM analysis were studied in three cases:
  a) Stagnation Cases ($V < 2$ ms^{-1}),
  b) Mild Ventilation Cases (2 ms$^{-1} \leq V \leq 5$ ms^{-1}),
  c) Strong Ventilation Cases ($V > 5$ ms^{-1})

  where V is horizontal wind speed.

BEGIN LAST LINE OF TEXT
BOTTOM OF IMAGE AREA, OUTSIDE DIMENSION FOR TABLES AND ILLUSTRATIONS
3/8"

EPA-287 (Cin.)
(4-76)

BEGIN FIRST LINE OF TEXT HERE
TYPING GUIDE SHEET
CENTER OF PAGE
TOP OF IMAGE AREA
DROPPED HEAD; BEGIN SECTIONS HERE

- The reliability of the CO analysis using the OVAM and a limited number of air pollution stations in the optimum network was determined to establish guidelines as to how many monitoring stations must be wind stations only and how many must observe both wind and air pollution.

- The effect of missing air pollution data in the optimum network was determined.

Due to limitations in the quantity of CO data available from the intensive field programs, an assessment of the OVAM using conventional statistical procedures was not possible. The research was conducted on a case study basis choosing cases that would represent extremes in the CO concentrations.

6 1/2"
9 1/8"
BEGIN LAST LINE OF TEXT
BOTTOM OF IMAGE AREA; OUTSIDE DIMENSION FOR TABLES AND ILLUSTRATIONS
3/8"

EPA-287 (Cin.)
(4-76)

TYPING GUIDE SHEET

MODEL DEVELOPMENT

MODEL EQUATIONS

Consider a volume encompassing an urban area. Observations of the pollution concentration, $\tilde{\psi}$, are given at various locations. The volume emissions density rate, Q(x,y), as well as the ambient wind velocity components, u, v, w (in the x, y and z directions, respectively) are also specified. The conservation equation for the pollutant, ψ, undergoing a first order decay in the atmosphere is

$$\frac{\partial \psi}{\partial t} + u\frac{\partial \psi}{\partial x} + v\frac{\partial \psi}{\partial y} + w\frac{\partial \psi}{\partial z} = K_H\left(\frac{\partial^2 \psi}{\partial x^2} + \frac{\partial^2 \psi}{\partial y^2}\right) + \frac{\partial}{\partial z}\left(K_z\frac{\partial \psi}{\partial z}\right) + Q - \tau\psi, \qquad (1)$$

where

ψ is the concentration (g/m^3),

K_H is the eddy diffusivity in the horizontal (m^2/s),

K_z is the eddy diffusivity in the vertical (m^2/s), and

τ is the decay rate (s^{-1})

The following assumptions are made:

1) $\psi(x,y,z) = \psi_o(x,y,0).g(z)$ where g(z) is the non-dimensional profile of ψ;

2) w = 0 in the layer between z = 0 and z = Z where Z is the top of the model;

3) Z is small (~ 50 m);

4) u and v do not vary substantially between their measurement height (~ 10 m) and Z.

When only surface (area) emissions were considered, g(z) was given as $\exp[(-\frac{1}{2}(z/S_z)^2]$. The concentration at Z was always less than the ground level concentration. When point sources with effective stack heights above and below Z are considered, concentrations at z may exceed the concentration at the ground, requiring a more flexible description of the concentration profile. Therefore:

TYPING GUIDE SHEET
BEGIN FIRST LINE OF TEXT HERE
CENTER OF PAGE
TOP OF IMAGE AREA

$$g(z) = 1.0 - K\,(z/Z)^2, \tag{2}$$

DROPPED HEAD; BEGIN SECTIONS HERE

where K is a parameter (positive or negative) to be determined.

Integrating (1) from z = 0 to Z, gives

$$\frac{\partial \hat{\psi}}{\partial t} = u\frac{\partial \hat{\psi}}{\partial x} + v\frac{\partial \hat{\psi}}{\partial y} + w\,\psi\Big|_0^Z = K_H \nabla_H^2 \hat{\psi} + K_z \frac{\partial \psi}{\partial z}\Big|_0^Z + QZ - \tau\hat{\psi}, \tag{3}$$

where

$$\hat{\psi} = \int_0^Z \psi\, dz,$$

and

$$\nabla_H^2 \hat{\psi} = \frac{\partial^2 \hat{\psi}}{\partial x^2} + \frac{\partial^2 \hat{\psi}}{\partial y^2}.$$

By Assumption 2,

$$w\psi\Big|_0^Z = 0 \tag{4}$$

The functional form of $\hat{\psi}$ becomes

$$\hat{\psi} = \psi_o(x,y,o) \int_o^Z g(z)\, dz = \psi_o G(Z), \tag{5}$$

where G (Z) = Z (1-K/3). The integral form of the vertical diffusion term is evaluated.

$$K_z \frac{\partial \psi}{\partial z}\Big|_Z = K\,(Z)\,\psi_o\,(x,y,0) \cdot \frac{dg}{dz}$$

$$= -K_z\,(Z)\,\psi_o(x,y,0) \cdot (2\kappa/Z) \tag{6}$$

BOTTOM OF IMAGE AREA; OUTSIDE DIMENSION FOR TABLES AND ILLUSTRATIONS
BEGIN LAST LINE OF TEXT
3/8"

EPA-287 (Cin.)
(4-76)

BEGIN FIRST LINE OF TEXT HERE
TYPING GUIDE SHEET
CENTER OF PAGE
TOP OF IMAGE AREA
DROPPED HEAD, BEGIN SECTIONS HERE

$$K_z \frac{\partial \psi}{\partial z}\bigg|_0 = 0 . \qquad (7)$$

Substitution of Eqs (4)-(7) into (3) gives:

$$G\left(\frac{\partial \psi_o}{\partial t} + u\frac{\partial \psi_o}{\partial x} + v\frac{\partial \psi_o}{\partial y}\right) - GK_H\nabla_H^2\psi_o + \frac{2\kappa}{Z}K_z(Z)\,\psi_o - QZ + \tau G\psi_o = 0. \qquad (8)$$

Since the observed concentrations are averaged values over a time increment, the time variability of the concentration over that increment cannot be accounted for. If the emissions data, Q, and the wind data are appropriate for that time interval, a near steady state (i.e., $\frac{\partial \psi}{\partial t} \cong 0$) may be assumed for the time interval. Applying that assumption, the emissions must be locally balanced by advection and diffusion. The assumption of a steady state is not a requirement of the analysis model. If only one set of observations is available, it is the best assumption. If data for more than one time are available, then the time variability can be included.

A dimensional analysis was applied to show the relative contribution of each term and to aid in computations by reducing truncation errors. The following definitions are formed.

$$\begin{aligned} \psi &= \bar{\psi}\cdot\psi', & K &= \bar{K}\cdot K', \\ x,y &= L\cdot(x',y'). & u,v &= \bar{U}\cdot(u',v'), \\ Q &= \bar{Q}\cdot Q', \end{aligned} \qquad (9)$$

where

$\bar{\psi}$ is a characteristic magnitude of ψ_o, (gm/m^3),

L is a characteristic length of the urban pollution system (m),

$\bar{Q}$ is a characteristic rate of emission density $(gm/m^3 s)$,

$\bar{U}$ is a characteristic wind speed (m/s),

and $\bar{K}$ is the characteristic magnitude of K_H or K_Z (m^2/s).

Substituting (9) into (8) gives

$$\frac{G\bar{U}\bar{\psi}}{L}\left(u'\frac{\partial \psi'}{\partial x'} + v'\frac{\partial \psi'}{\partial y'}\right) - \frac{G\bar{K}\bar{\psi}}{L^2}\left(K_H'\nabla_H^2\psi'\right) + \frac{2\kappa\bar{K}\bar{\psi}}{Z}\,\psi' - \bar{Q}Z\,(Q') + \tau G\bar{\psi}\,\psi' = 0 \qquad (10)$$

BOTTOM OF IMAGE AREA, OUTSIDE DIMENSION FOR TABLES AND ILLUSTRATIONS
BEGIN LAST LINE OF TEXT
3/8"

EPA-287 (Cin.)
(4-76)

BEGIN FIRST LINE OF TEXT HERE
TYPING GUIDE SHEET
CENTER OF PAGE
TOP OF IMAGE AREA
DROPPED HEAD: BEGIN SECTIONS HERE

Dividing (10) by $\frac{D\bar{\psi}G}{L}$ and dropping the prime (') from the non-dimensional variables, gives

$$u\frac{\partial\psi}{\partial x} + v\frac{\partial\psi}{\partial y} - R(K_H\nabla_H^2\psi) + \zeta\,\psi - \eta\,Q = 0 \qquad (11)$$

where

$$R = \bar{K}/\bar{U}L,$$

$$\eta = (L\bar{Q}Z/G\bar{U}\bar{\psi}),$$

$$\zeta = \frac{2\kappa\bar{K}}{G\bar{U}Z} + \frac{\tau L}{\bar{U}},$$

The advection terms, $u\frac{\partial\psi}{\partial x}$, and $v\frac{\partial\psi}{\partial y}$, are on the order of unity and the other terms are scaled by the non-dimensional coefficients. The magnitude of the non-dimensional coefficients determines the relative contribution of each term of the equation. It was shown in VBC that R<<1; therefore

$$A = u\frac{\partial\psi}{\partial x} + v\frac{\partial\psi}{\partial y} + \zeta\psi - \eta\,Q \cong 0. \qquad (12)$$

Eq. (12) is identical in form to the constraint equation in VBC. The only difference occurs in the definition of ζ. Following the developemnt VBC, the Euler-Lagrange equation that minimizes the error variance is

$$\tilde{\alpha}\,(\psi - \tilde{\psi}) + \alpha\left(\zeta A - \frac{\partial uA}{\partial x} - \frac{\partial uA}{\partial y}\right) = 0 \qquad (13)$$

Substituting (12) into (13) and combining terms leads to the following form of the Euler-Lagrange equation:

$$u^2\frac{\partial^2\psi}{\partial x^2} + 2uv\frac{\partial^2\psi}{\partial x\partial y} + v^2\frac{\partial^2\psi}{\partial y^2} + \frac{\partial\psi}{\partial x}\left(\frac{\partial u^2}{\partial x} + \frac{\partial uv}{\partial y}\right) + \frac{\partial\psi}{\partial y}\left(\frac{\partial v^2}{\partial x} + \frac{\partial uv}{\partial x}\right) - \qquad (14)$$

$$(\zeta^2 + \tilde{\alpha}/\alpha)\,\psi = -\tilde{\alpha}/\alpha\,\tilde{\psi} - \eta\,(\zeta Q - u\frac{\partial Q}{\partial x} - v\frac{\partial Q}{\partial y}).$$

In order to obtain a solution to eq. (14), the spatial distributions of the wind components (u,v), observed concentration ($\tilde{\psi}$), the relative weights ($\tilde{\alpha}/\alpha$), the decay rate (τ), the profile parameter (K), and the sources (Q) are required.

BEGIN LAST LINE OF TEXT HERE
BOTTOM OF IMAGE AREA. OUTSIDE DIMENSION FOR TABLES AND ILLUSTRATIONS
3/8"

EPA-287 (Cin.)
(4-76)

BEGIN FIRST LINE OF TEXT HERE
TYPING GUIDE SHEET
CENTER OF PAGE
TOP OF IMAGE AREA
DROPPED HEAD; BEGIN SECTIONS HERE

STUDY AREA

The OSN grid for the St. Louis area was centered at UTM coordinates of 738.5 km Easting, 4279.8 Northing (the intersection of Lindell Blvd. with Kings highway). The area emissions inventory, developed by EPA, is designated in 1.0 km or larger increments, and is coincident with the UTM coordinate system. Rather than make the emissions inventory conform to the OSN grid, the center of the grid for these analyses was shifted to 738.0 km E and 4279.0 km N. The analysis area and the OSN network are shown in Figure 2. A 20 km x 20 km regular grid with 1 km spacing (thus, 441 grid points) was adopted for the tests of the OVAM. The sources are normalized to a 1 km^2 area.

POINT SOURCES

Operationally, only the point sources of CO that emit more than 50 kg/hr are used in the analysis. These account for approximately 98 percent of point source emissions of CO in the summer and reduces the number of sources from 200 to about 20. The point sources are further stratified into those with effective source heights (stack height plus plume rise) above the top of the model (Z) and those below.

The effects of each point source are included by establishing the upper and lower boundary concentrations and the concentration profile. Some point sources have an effective emission height (stack height plus plume rise) greater than the top of the modeled volume (~ 50 m). Those sources do not occur in the volume and are not included in the source term, but are included in the analysis indirectly through the estimation of the profile parameter. The remaining point sources are smoothed over the grid square and are included as area sources in the constraint (continuity) equation because the equation does not discriminate among source types.

The consequence of this treatment is demonstrated in Figure 3 by considering two such point sources having different stack heights but otherwise identical emission characteristics placed in a uniform air flow field with a minimal background. The greatest impact of the source below the top of the model is in the immediate surroundings. The analysis creates an anomalous negative concent on upwind of the source and overpredicts the concentration in the fir kilometers downwind of the source (this feature was shown and discussed . If the source is above the top of the model, and not considered by the alysis, the location and magnitude of the maximum are predicted nearly correctly. Clearly, the inclusion of the point source, as an area source in the analysis equation, creates a problem for this analysis technique.

PROFILE PARAMETER

The profile parameter, K, is obtained by estimating the concentration at the ground, $\psi(x,y,0)$, and at the top of the volume, $\psi(x,y,Z)$, at each grid point from the point and area sources. The value is determined using the definition of K from eq. (2) i.e.,

$$K = 1.0 - (\psi(x,y,Z)+\psi_B)/(\psi(x,y,0)+\psi_B)$$

BEGIN LAST LINE OF TEXT HERE
BOTTOM OF IMAGE AREA; OUTSIDE DIMENSION FOR TABLES AND ILLUSTRATIONS
3/8"

EPA-287 (Cin.) (4-76)

BEGIN FIRST LINE OF TEXT HERE
TYPING GUIDE SHEET
CENTER OF PAGE
TOP OF IMAGE AREA
DROPPED HEAD: BEGIN SECTI HERE

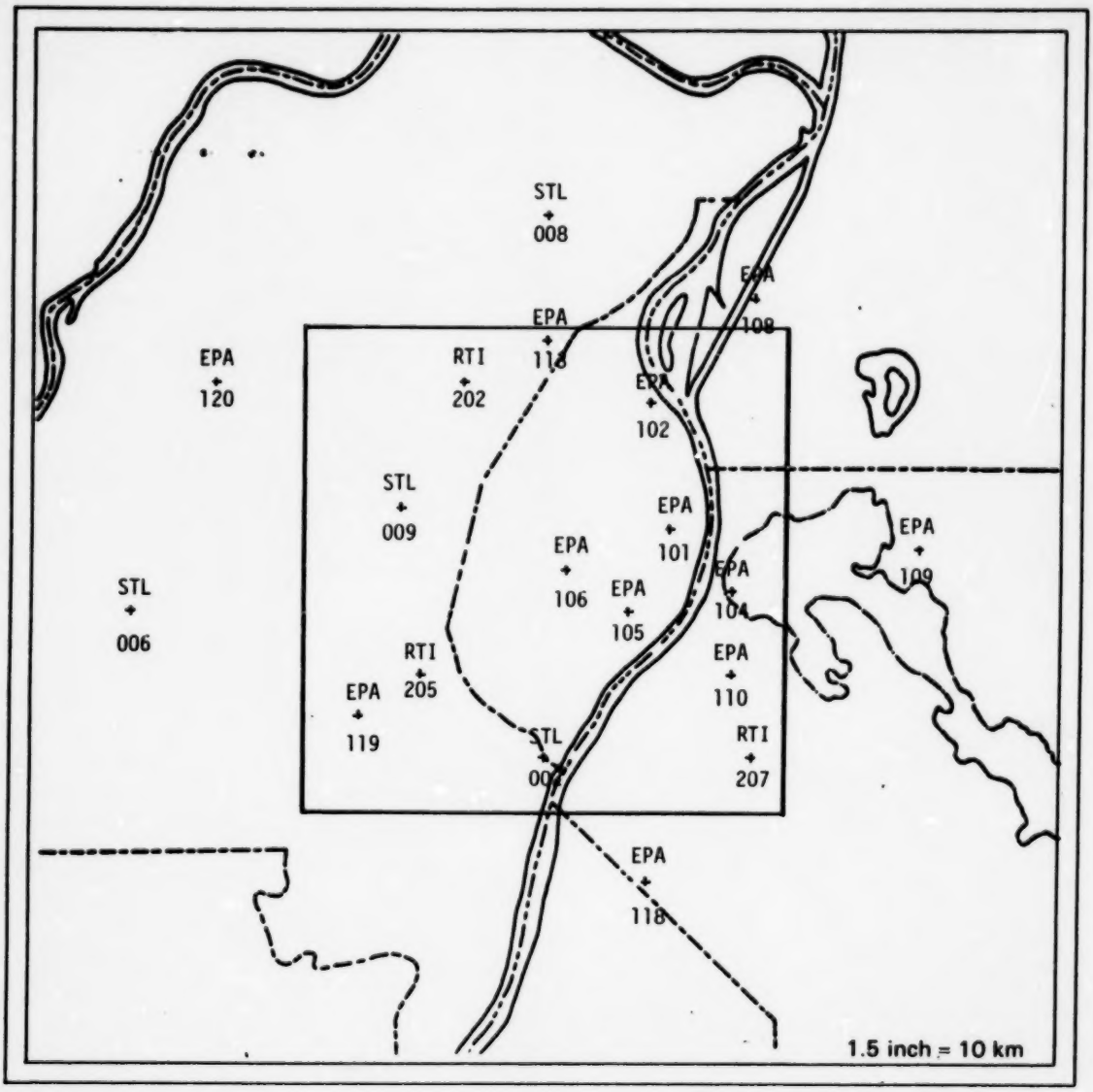

Figure 2. OSN network and OVAM analysis area.

BEGIN LAST LINE OF TEXT
3/8"
BOTTOM OF IMAGE AREA, OUTSIDE DIMENSION FOR TABLES AND ILLUSTRATIONS

EPA-287 (Cin.)
(4-76)

BEGIN FIRST LINE OF TEXT HERE
TYPING GUIDE SHEET
CENTER OF PAGE
TOP OF IMAGE AREA
DROPPED HEAD: BEGIN SECTIONS HERE

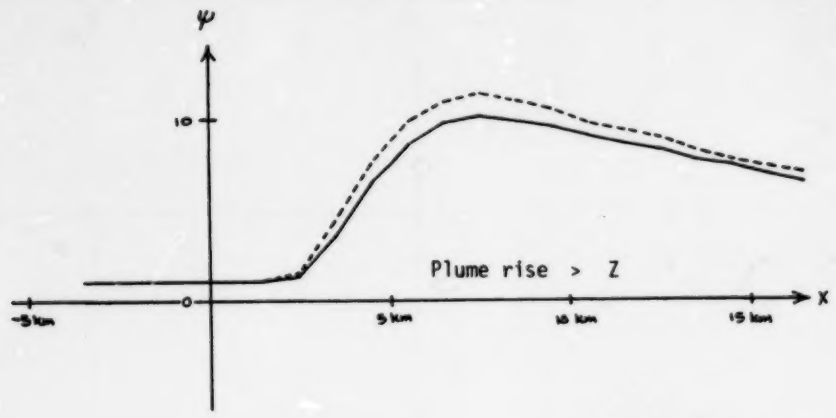

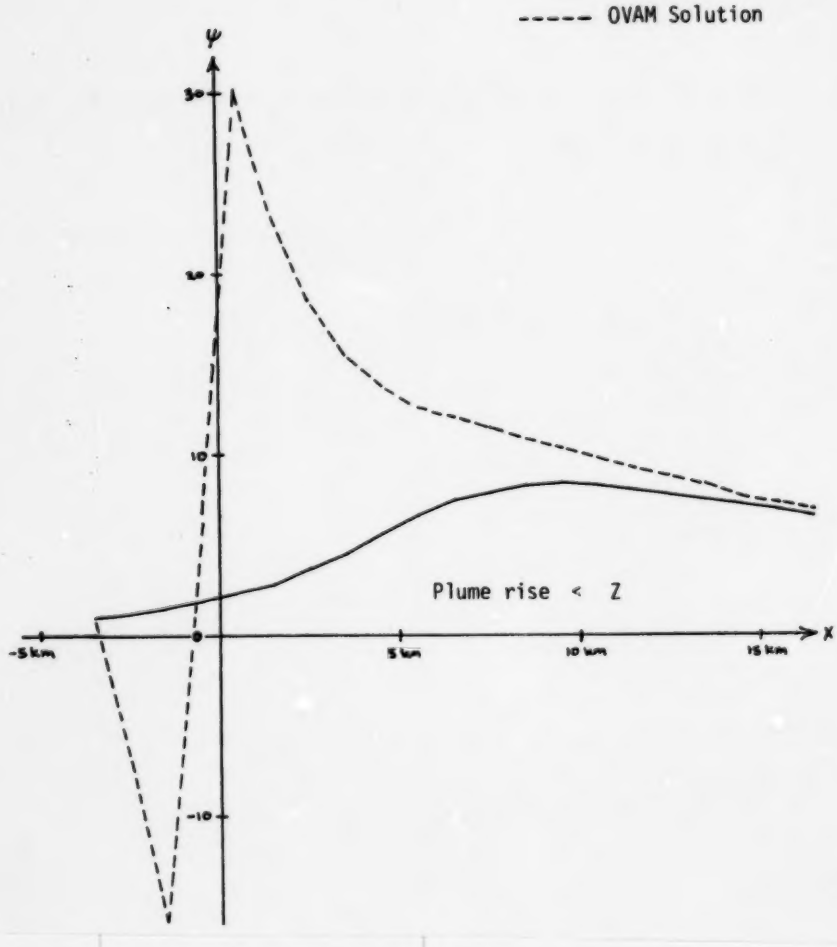

Figure 3. Response of OVAM analysis to point source plume rise above and below the top of the model, Z.

BEGIN LAST LINE OF TEXT
BOTTOM OF IMAGE AREA, OUTSIDE DIMENSION FOR TABLES AND ILLUSTRATIONS
3/8"

EPA-287 (Cin.)
(4-76)

where ψ_B is a background value of ψ. Concentration estimates at the ground and model top are carried out for area and point sources independently, using a modified version of the RAM dispersion model (Novak and Turner, 1976). Plume rise is based on source parameters, wind speed, stability, and ambient temperature. The computations are extracted from the plume rise coding of the RAM model.

AEROMETRIC DATA

The 19 station OSN and eight additional stations provided data for this study (Figure 1). The data consisted of five-minute average values from the EPA and RTI stations and three-minute average values from the St. Louis city/county stations. Five-point running averages centered about the hour and half-hour were computed. At least three of the five readings were required for a valid average. The averaging period is consistent with the averaging performed in the hydrodynamic model which produced the simulated wind fields upon which the OSN was based.

All CO concentrations were measured at 10 m. Winds were measured at 10 m at the three RTI stations, the St. Louis city/county stations, and three RAPS stations (EPA 108, EPA 110 and EPA 118). Measurements at the remaining 13 RAPS stations were made at the 30-m level. Those data were extrapolated downward to 10 m using the procedure described in Volume II (Vukovich and Clayton, 1979).

OBJECTIVE ANALYSIS

The OVAM formulation assumes that the winds and concentration, $\tilde{\psi}$, are known throughout the domain of interest. In reality, they are known at a few scattered observation points. Estimates of the winds and concentration at each grid point were determined using the procedure developed by Barnes (Appendix A) which uses an exponential weighting function to interpolate the value for a grid point from nearby observation. The interpolated values are corrected, based on the error of the interpolation at the observation points using an exponential weight function that is more restrictive in its area of influence.

The Barnes analysis produced initial values at the 441 grid points in the model. The non-dimensional concentrations were determined by dividing the initial concentration by $\bar{\psi}$ (see equation 9). The concentration, $\bar{\psi}$, was defined as the mean value of the 441 interpolated grid values.

RELAXATION PROCEDURE

The analysis equation (14) was solved using the sequential over-relaxation (Liebmann) technique outlined in Thompson (1962). Previous experience (VBC) indicated that a solution could be attained using point-to-point relaxation. The Liebmann procedure was used to speed convergence.

The analysis produces negative concentration estimates in regions upwind of sources where observed contentrations were small. While that result is consistent with the mathematics of the analysis model and was found in VBC, it is physically unrealistic. Two additional requirements to the analysis have

BEGIN FIRST LINE OF TEXT HERE
TYPING GUIDE SHEET
CENTER OF PAGE
TOP OF IMAGE AREA
DROPPED HEAD. BEGIN SECTIONS HERE

overcome the problem. A "background" concentration was subtracted from all $\tilde{\psi}$ estimates from the Barnes analysis. The background concentration was the larger of two potential values: a) the smallest concentration from the Barnes analysis or b) one-half the minimum detectable concentration of the instrumentation (0.1 ppm or $\sim 1.15 \times 10^{-4}$ gm/m^3). The relaxation procedure was programmed to set negative values to zero as they were encountered. Because of this condition, the relaxation criteria (that the increment of normalized concentration was less than 0.01) was not always satisfied at every grid point within the array. Grid points in areas of very small emissions that are upwind of larger sources were particularly affected. However, small concentrations were expected in these areas, so forcing the procedure to meet the solution conditions had little impact upon the larger concentrations elsewhere.

The number of "unrelaxed" points reached a constant value after several iterations. The number of such points generally equaled the number of "zero points". The change in the mean square error was small, and the solution was attained when the number of unrelaxed points was less than ten and constant for three iterations. Otherwise, the procedure was executed 30 times. In some cases, the number of unrelaxed points was greater than nine but a steady error variance was achieved, i.e., more iterations would not achieve a reduction in the error variance. After the relaxation solution was achieved, the background concentration was added to the analysis.

OPTIONS

Application of the OVAM to a realistic situation leaves several options or decisions for the user. The boundary conditions and the relative weights of the observations and constraint equation ($\tilde{\alpha}/\alpha$) are user-specified. The manner of treatment of point sources is also an optional feature. Each choice will affect the solution.

Boundary Conditions

The variational analysis gives two options to boundary conditions. The fixed condition, $\delta\psi = 0$, means that ψ is not permitted to vary at the boundary. The initial boundary values are obtained through the Barnes algorithm and these are by no means exact.

The other boundary condition, $\delta\left(\frac{\partial \psi}{\partial n}\right) = 0$, means that the gradient normal to the boundary does not change during the relaxation procedure. This condition was interpreted so that the normal gradient given by the Barnes analysis varied spatially but not with iteration. This approach occasionally resulted in large unjustifiable concentration gradients at the boundaries. The subsequent OVAM analyses produced negative concentrations at the boundaries which adversely affected the analyses at interior grid points near the boundary. The problem was most acute at inflow boundaries where emissions were very small.

The open boundary condition does not specify the gradient; rather it specifies that it cannot change. As a result of experience, the open boundary condition was adopted for the OVAM analysis in the following form:

BEGIN LAST LINE OF TEXT
BOTTOM OF IMAGE AREA, OUTSIDE DIMENSION FOR TABLES AND ILLUSTRATIONS
3/8"

EPA-287 (Cin.)
(4-76)

BEGIN FIRST LINE OF TEXT HERE
TYPING GUIDE SHEET
CENTER OF PAGE
TOP OF IMAGE AREA
DROPPED HEAD: BEGIN SECTIONS HERE

$$\frac{\partial \psi}{\partial n} = \begin{cases} 0 & \text{at inflow boundaries} \\ \frac{\partial \tilde{\Psi}}{n} & \text{at outflow boundaries} \end{cases}$$

where $\tilde{\Psi}$ is the Barnes analysis. This formulation does not permit mass inflow from sources outside the modeled region, but mass can be lost by outflow. Hence, mass is not fully conserved in the OVAM. While there can be wide discussion of various modifications of the open boundary conditions, these conditions gave more reasonable results than the others tested.

Ratio of Weights

The choice of the value given to the weight for the interpolated concentration, $\tilde{\alpha}$, and to the weight for the constraint equation, α, has been shown (VBC) to have significant influence on the analysis. Increasing the weight given to the constraint equation (decreasing $\tilde{\alpha}/\alpha$) in areas without observations made the OVAM analysis much more compatible with the analytic solution, and the error variance was substantially reduced.

The weights can be interpreted as measures of the user's confidence that an observation is "representative" of the concentration within a given distance of the observing point. At grid points adjacent to observation point, the interpolated concentration should be similar to the observaton. At more distant grid points, the interpolated value may not be dependent upon the nearest observation.

Chaney (1979) studied variations in CO concentrations within a one km radius of selected RAPS surface monitoring stations. He showed very poor correlation (r = 0.10) of area averaged concentrations with an urban RAPS station. At a rural RAPS site, the correlation was 0.80 principally because of lower concentrations. The mean percentage difference of area averaged concentrations and concentrations at the RAPS site was about -35 percent in both urban and rural sites. Ott (1977), Ott and Eliassen (1973), and Ludwig and Kealoha (1975) address the problem of CO variability in street canyon and urban areas. They show 200 or 300 percent concentration changes by changing sampling location by less than 100 m.

The value of $\tilde{\alpha}$ or α is not significant to the resultant analysis, but the ratio $\tilde{\alpha}/\alpha$ is. To provide an opportunity to examine the effects of the results upon the distance of the grid point from the nearest observing location, d, the ratio $\tilde{\alpha}/\alpha$ was given the form:

$$\tilde{\alpha}/\alpha = \begin{cases} 100, & d/RAD < 0.1 \\ 1.0/(ALFA \cdot (d/RAD)^2), & 0.1 \leq d/RAD \leq 1.0 \\ 1.0/ALFA, & d/RAD > 1.0. \end{cases}$$

BEGIN LAST LINE OF TEXT HERE
BOTTOM OF IMAGE AREA, OUTSIDE DIMENSION FOR TABLES AND ILLUSTRATIONS
3/8"

EPA-287 (Cin.) (4-76)

BEGIN FIRST LINE OF TEXT HERE
TYPING GUIDE SHEET
CENTER OF PAGE
TOP OF IMAGE AREA
DROPPED HEAD; BEGIN SECTIONS HERE

where d is the distance to the nearest observation, but less than RAD, the radius of influence of a point. Thus, the weight is dependent on RAD and a given value, ALFA, as shown in Figure 4. In this case, RAD = 2.5 km. The choice of the RAD is large in view of Chaney's data. However, the area emissions data are known to one-km square, so the minimum detectable scale of variability due to source influence is two km. At that distance, $\tilde{\alpha}/\alpha \sim 0.2$ with the choice of RAD and ALFA. Since $\tilde{\alpha}/\alpha$ is not made a function of land use (e.g., urban, suburban, or rural), the choice was a reasonable compromise.

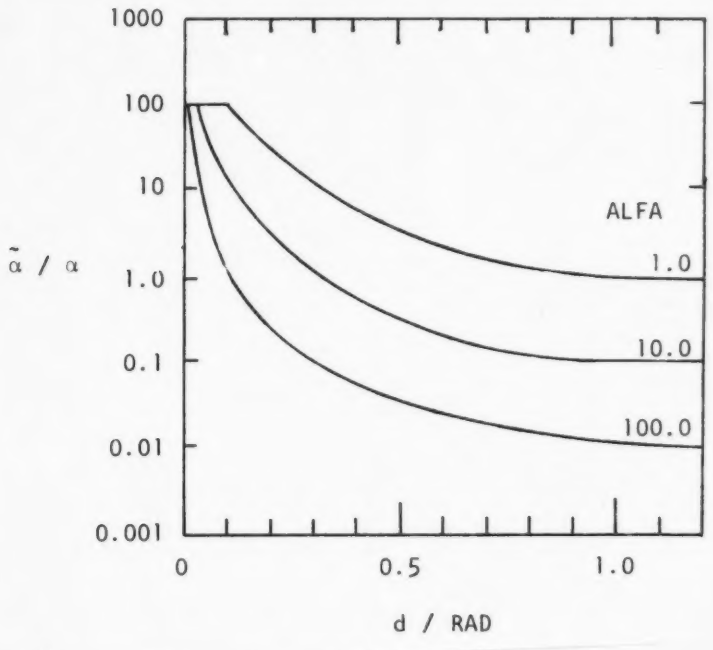

Figure 4. Ratio of weights, $\tilde{\alpha}/\alpha$, as a function of ALFA and RAD.

BEGIN LAST LINE OF TEXT HERE
BOTTOM OF IMAGE AREA OUTSIDE DIMENSION FOR TABLES AND ILLUSTRATIONS
3/8"

BEGIN FIRST LINE OF TEXT HERE
TYPING GUIDE SHEET
CENTER OF PAGE
TOP OF IMAGE AREA
DROPPED HEAD; BEGIN SECTIONS HERE

MODEL APPLICATIONS

SELECTION OF CASES

Besides the criteria mentioned in the Introduction, an additional criterion was applied for the selection of case studies. Valid wind and CO data were required at 13 of the 19 OSN locations. The criterion was based on the order of variability of the wind field in St. Louis which requires a minimum of 13 stations to be accurately specified (VBC). It was assumed that the CO distribution had at least the same order of variability as the wind field, thus requiring a minimum of 13 observations from the OSN. Case studies were selected after the wind and CO data were screened using hourly plots for each station (Figure 5). Criteria for ventilation were based on wind speeds at the National Weather Service station, Lambert Field (Figure 1).

In August 1975, the CO concentrations were small and showed little variation. Winds were usually from the southwest. August 12 from 1100 to 1800 CST was chosen for analysis. Wind speeds between 5 and 7 m/s were reported (i.e., strong ventilation). In February 1976, the CO concentration showed more variability in time and in space. Several short periods qualify for analysis. February 18 from 1800 to 2100 was chosen because the larger CO concentrations were about the highest found during the winter when there were sufficient data, and because the winds were 3 to 4 m/s (i.e., moderate ventilation). February 26 from 1800 to 2300 CST was chosen because the winds were light and variable (i.e., mild ventilation). The last case, February 27, a weekday, from 0000 to 0800 CST, was chosen to observe the decreasing CO during the night and increasing CO during morning rush hour.

MODEL PERFORMANCE

The consequences of the OVAM can be understood by first considering the Barnes analysis (Figure 6), which was performed without considering the winds. Within the network, the resultant wind was from the south-southwest at 2.5 m/s. The Lambert Field winds were westerly at 5.2 m/s. Nearly one-half the observations used to determine the resultant wind over the network were made in the central portion of the city where surface roughness and "heat island" effects reduce the wind speed. Consequently, the resultant wind speed is generally smaller than the wind speed at Lambert Field. The Barnes analysis and the CO observations showed small variations over the domain. CO ranged from 500 ppb in the southwest to 80 ppb in the southeastern quarter. The OVAM analysis changed the Barnes analysis along the southern border where CO concentrations increased substantially in a narrow finger

BEGIN LAST LINE OF TEXT
BOTTOM OF IMAGE AREA OUTSIDE DIMENSION FOR TABLES AND ILLUSTRATIONS
3/8"

EPA-287 (Cin.) (4-76)

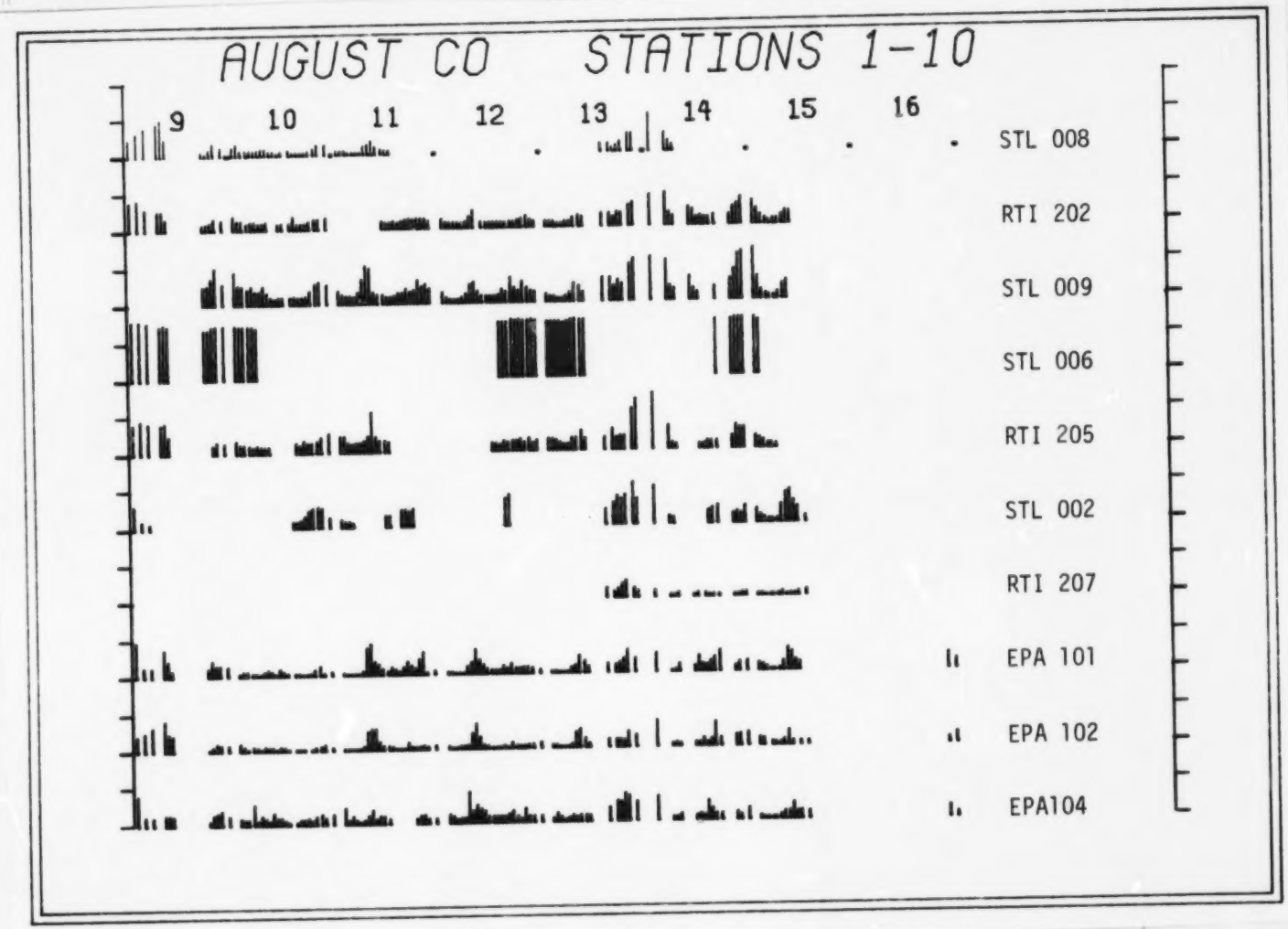

Figure 5. Hourly CO concentrations at OSN locations, August 9 to 16, 1975 and February 14 to 29, 1976. Vertical tick increment is 5 ppm.

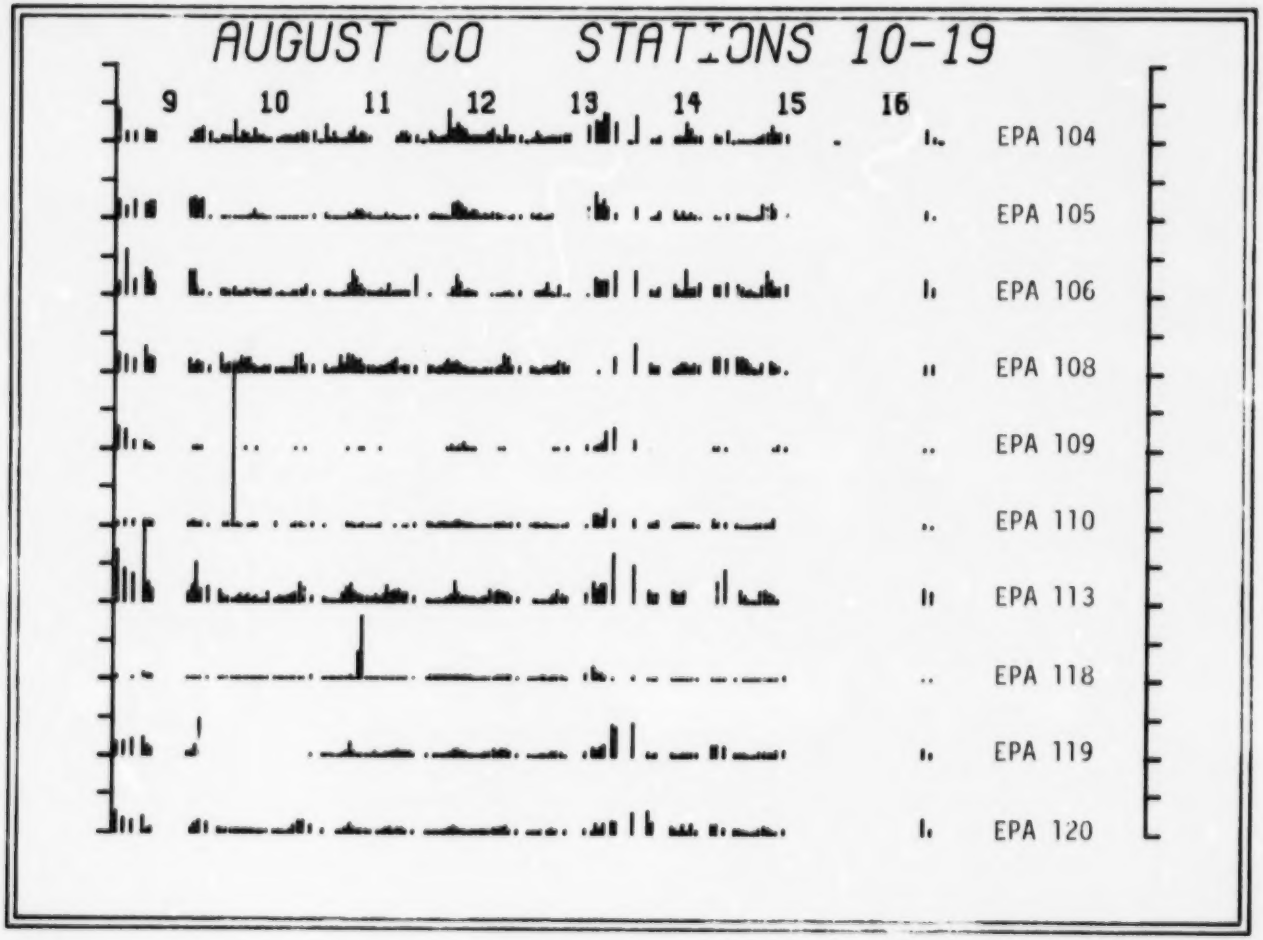

Figure 5. (continued)

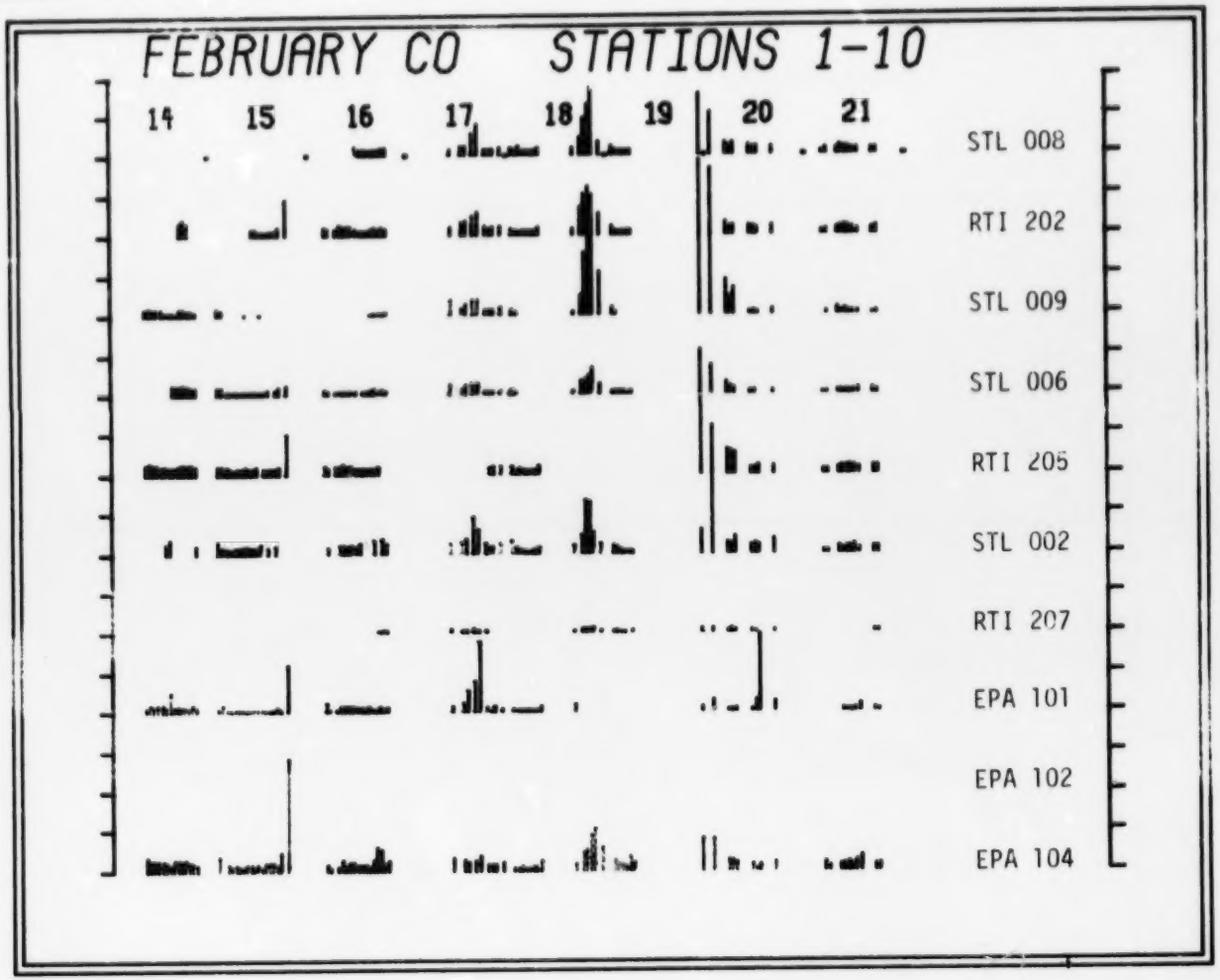

Figure 5. (continued)

TYPING GUIDE SHEET
BEGIN FIRST LINE OF TEXT HERE
CENTER OF PAGE
TOP OF IMAGE AREA
DROPPED HEAD. BEGIN SECTIONS HERE

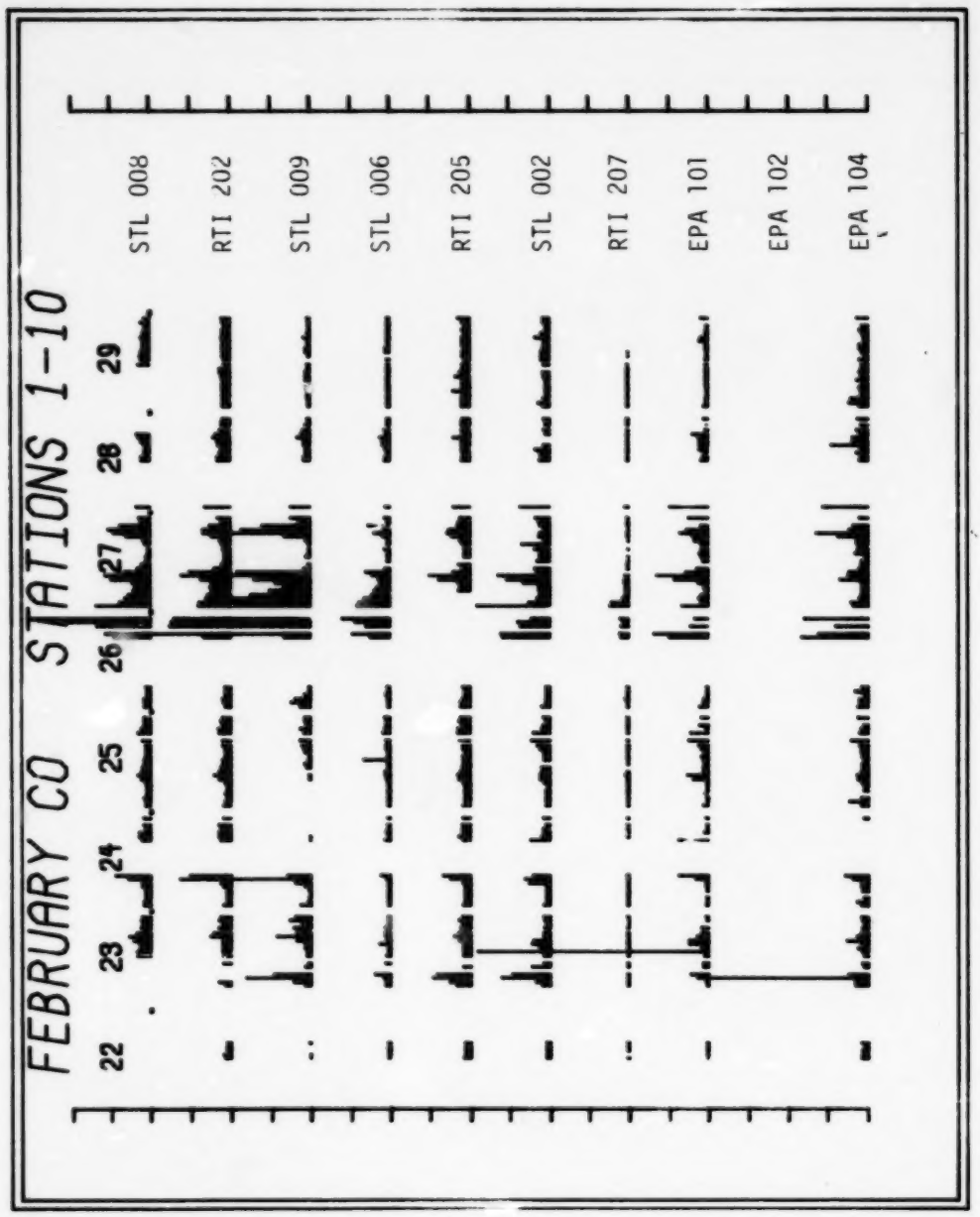

Figure 5. (continued)

BEGIN LAST LINE OF TEXT
3/8"
BOTTOM OF IMAGE AREA. OUTSIDE DIMENSION FOR TABLES AND ILLUSTRATIONS

EPA-287 (Cin.)
(4-76)

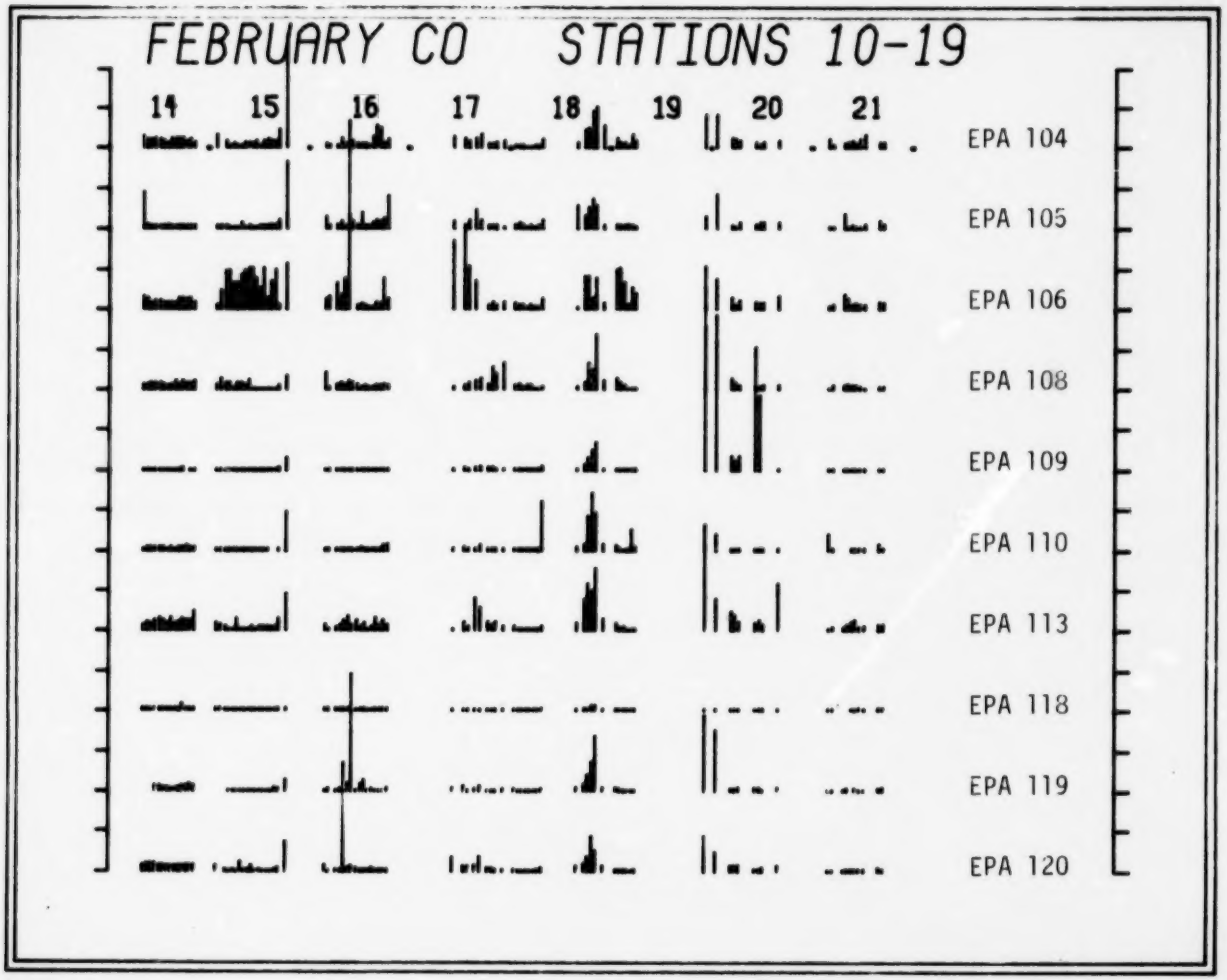

Figure 5. (continued)

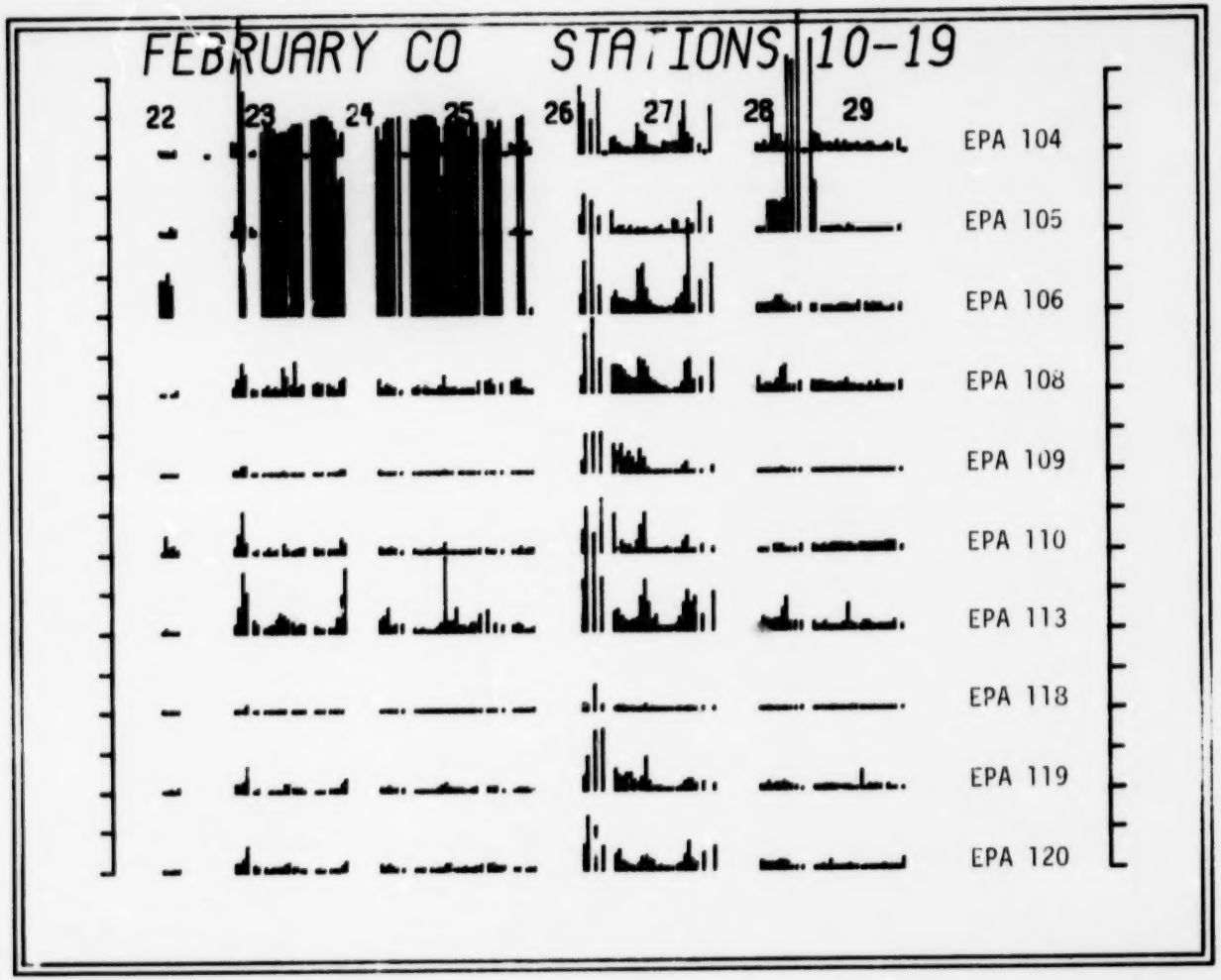

Figure 5. (continued)

BEGIN FIRST LINE OF TEXT HERE
TYPING GUIDE SHEET
CENTER OF PAGE
TOP OF IMAGE AREA
DROPPED HEAD; BEGIN SECTION HERE

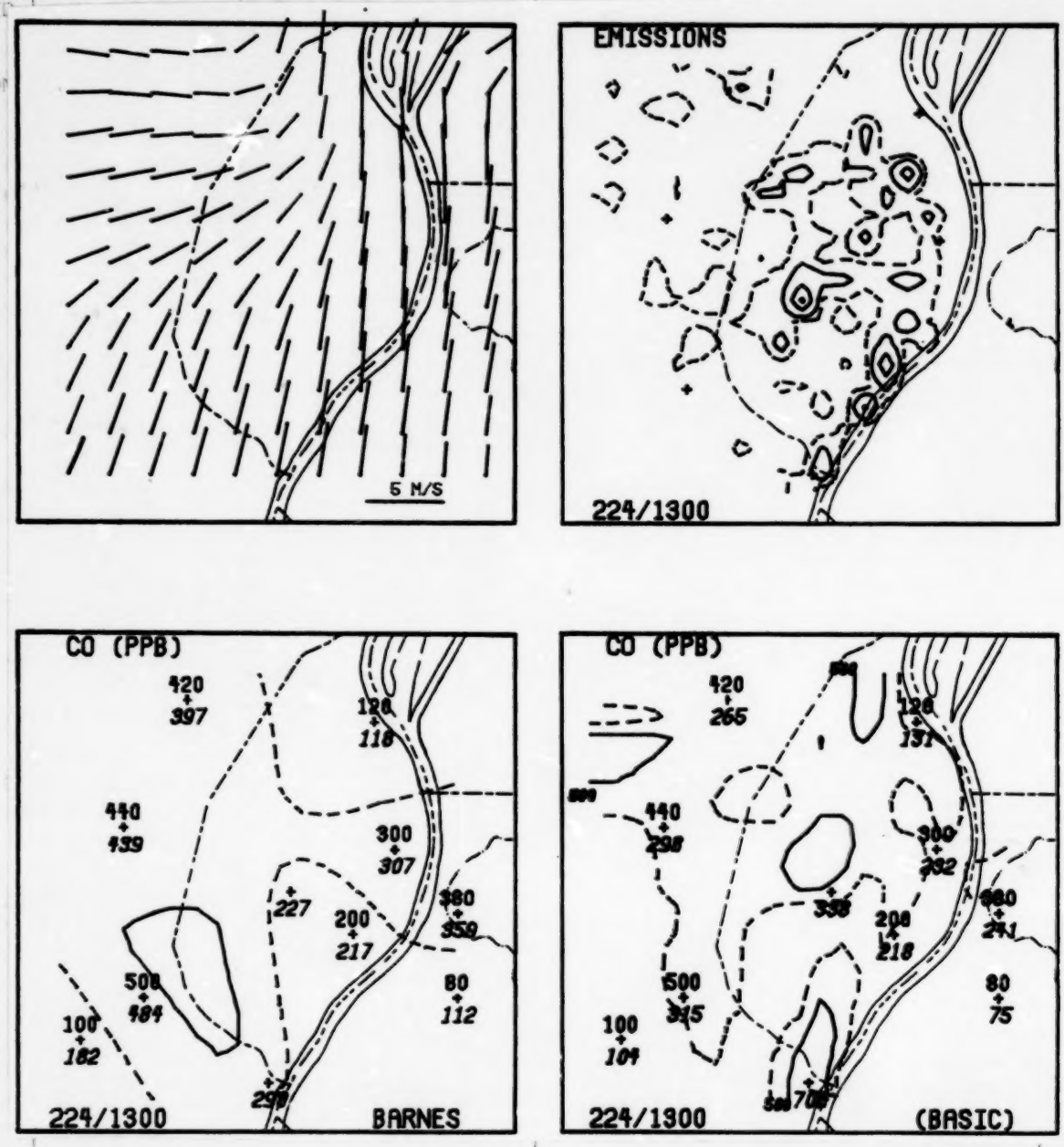

Figure 6. Wind vectors, area sources, and CO isopleths, August 12, 1975 at 1300 CST. Source isopleths are in increments of Q. Observed concentrations are plotted above the station mark (+); interpolated values at nearest grid point, below the mark.

BEGIN LAST LINE OF TEXT
BOTTOM OF IMAGE AREA; OUTSIDE DIMENSION FOR TABLES AND ILLUSTRATIONS
3/8"

EPA-287 (Cin.)
(4-76)

BEGIN FIRST LINE OF TEXT HERE
TYPING GUIDE SHEET
CENTER OF PAGE
TOP OF IMAGE AREA
DROPPED HEAD: BEGIN SECTIONS HERE

extending along the local wind direction and downwind of the larger emissions. The Barnes analysis interpolated a value of 430 ppb at the grid point adjacent to the missing location, but the OVAM increased that concentration to 755 ppb. The OVAM developed several other maxima near the center of the grid that are unsupported by the observations, but where the emissions were large.

Centers are justified by being located downwind of principal source regions. The relative minimum, upwind of the sources, a common feature of the OVAM, occurs because the analysis tends to suppress concentration estimates (VBC). Since the observations are several kilometers away from this area, the constraint equation is dominant ($\tilde{\alpha}/\alpha \cong 0.1$) and is attempting to conserve mass in that local area. The increase in mass (concentration) downwind is compensated by a reduction in mass upwind of the source. The amount of reduction is related to the along-wind gradient of emission rate.

The concentration in the north-northeastern and northwest sections also increases in response to the emissions. Thus, the wind and emission patterns of the area have a major impact upon OVAM results. The concentration estimates are changed dramatically at EPA 106 (from 181 to 327 ppb) and at EPA 102 (from 107 to 208 ppb). Both stations were downwind of large sources, contributing to an increase even though $\tilde{\alpha}/\alpha \sim 1.0$ near the stations. Furthermore, the predicted concentration gradient is large in that area, so the displacement of the grid point from the observation is important.

MODEL SENSITIVITY

The ratio $\tilde{\alpha}/\alpha$ and Z, the depth of the volume, have been shown to be particularly influential in the OVAM analysis (VBC). In the present development, with point sources included and with questions as to the correlation of nearby concentrations to the measured concentrations, the selection of Z and $\tilde{\alpha}/\alpha$ and of RAD, the maximum radius of the observation's influence, are important. The impact of these user-defined parameters was examined using the data for August 12, 1975 at 1300 CST (1400 CDT). The values of the three parameters in the basic (reference) case and the test cases are given in Table 1. The studies were carried out a) using the initial distribution of Ψ and the wind field developed using the Barnes analysis with interpolation along the wind vector, and b) without the influence of the local wind vector. The difference of results between cases was minor due to small wind speeds, so only the case (b) results are given. Effects were shown by computing the percentage change of the concentrations (Figure 7) with the varied conditions related to the basic condition. Differences are also examined along the south to north line, approximately in the direction of the wind, 12 km from the western edge of the domain (Figure 8). All of the features of the analyses do not occur along the line, but salient features can be illustrated.

The cross section analysis (Figures 8) clearly shows that the choice of ALFA is the primary factor in changing the concentration estimates. When ALFA is reduced to 5, the concentration changes are small and negative. When ALFA increases, the impact of sources upon the analysis increases and all values of concentration increase. The concentration gradient along the cross section for all curves is essentially the same for the first 10 km, but increases more rapidly for the next two km (for ALFA > 10) in response to strong area sources just to the west. There are changes in the gradient in response to emissions further north. For the smaller value of ALFA (5.0), the gradient shows

BEGIN LAST LINE OF TEXT
BOTTOM OF IMAGE AREA, OUTSIDE DIMENSION FOR TABLES AND ILLUSTRATIONS

EPA-287 (Cin.) (4-76)

BEGIN FIRST LINE OF TEXT HERE
TYPING GUIDE SHEET
CENTER OF PAGE
TOP OF IMAGE AREA
DROPPED HEAD; BEGIN SECTIONS HERE

TABLE 1. PARAMETERS OF SENSITIVITY ANALYSIS

Test	ALFA	RAD	Z	Test	ALFA	RAD	Z
BASIC	10	2.5	50	4	10	5.0	50
1	5	2.5	50	5	10	1.5	50
2	50	2.5	50	6	10	2.5	100
3	100	2.5	50	7	10	2.5	200

similar trends away from sources and responds less to the sources than does the basic case.

The higher values of ALFA increase concentrations when emissions are large. The initial, upwind difference among the concentrations is due to the strong source region at the upwind (south) boundary. The principal response seems to occur in areas where the actual emissions are two or more times larger than the average emissions over the total analysis area.

Changing RAD from 1.5 to 5.0 has little effect upon the concentrations. The smaller value produced the least change. The larger value produced a decrease in the concentration toward the north (Figure 8) in response to the influence of a nearby observation and to a lesser degree in response to nearby sources. The same feature is shown in the percentage change (Figure 7) in concentration at the northern border of the area.

Increasing Z produces a much smoother analysis along the cross section, because the pollution is being averaged over a much deeper layer and the effects of the vertical profile are much smaller, thereby decreasing the effects of strong area sources. Upwind of sources, the percentage change exceeds 200 percent and the concentrations have increased, because the influence of a strong gradient associated with area sources has been reduced by averaging the emissions over a deeper volume.

The results of the sensitivity analysis shows that the choice of ALFA has the primary impact upon the OVAM analysis. The initial concentration has little impact upon the choice of the parameter. Larger values of Z smooth the analysis, de-emphasizing the source. The analyses are least sensitive to the choice of RAD.

TIME SEQUENCE OF ANALYSES: 12 AUGUST 1975

At 1100 and 1200 CST on 12 August, the winds were westerly to southwesterly over much of the area. A concentration maxima developed along

BEGIN LAST LINE OF TEXT
BOTTOM OF IMAGE AREA, OUTSIDE DIMENSION FOR TABLES AND ILLUSTRATIONS
3/8"

EPA-287 (Cin.)
(4-76)

BEGIN FIRST LINE OF TEXT HERE
TYPING GUIDE SHEET
CENTER OF PAGE
TOP OF IMAGE AREA
DROPPED HEAD; BEGIN SECTION HERE

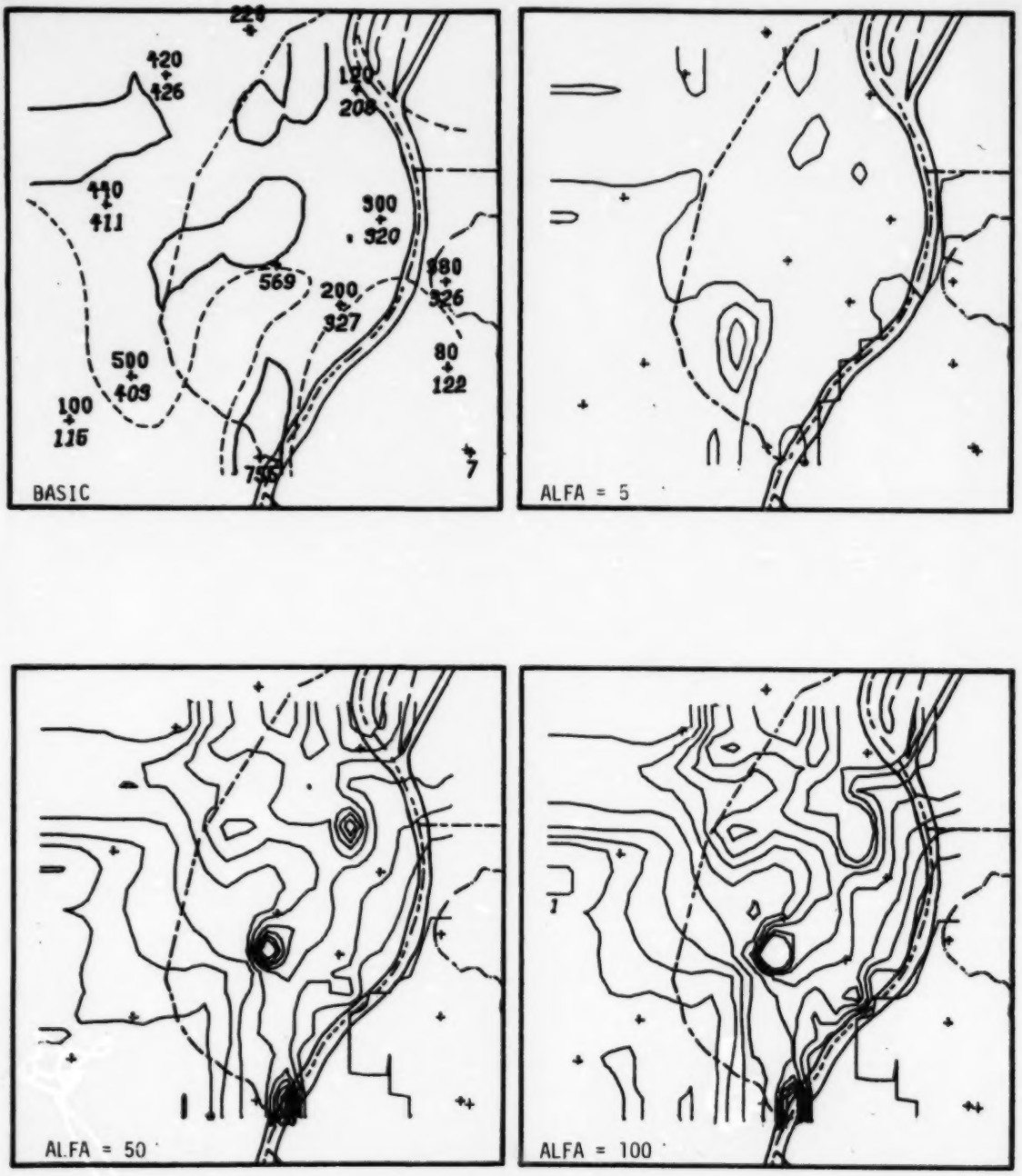

Figure 7. Isopleths of CO concentration for basic state of sensitivity analyses and isopleths of percent change from basic state (interval 33%) induced by indicated parameter value. Zero percent change isopleth is indicated.

BEGIN LAST LINE OF TEXT
BOTTOM OF IMAGE AREA; OUTSIDE DIMENSION FOR TABLES AND ILLUSTRATIONS
3/8"

EPA-287 (Cin.)
(4-76)

BEGIN FIRST LINE OF TEXT HERE
TYPING GUIDE SHEET
CENTER OF PAGE
TOP OF IMAGE AREA
DROPP HEAD BEGIN SECTI HERE

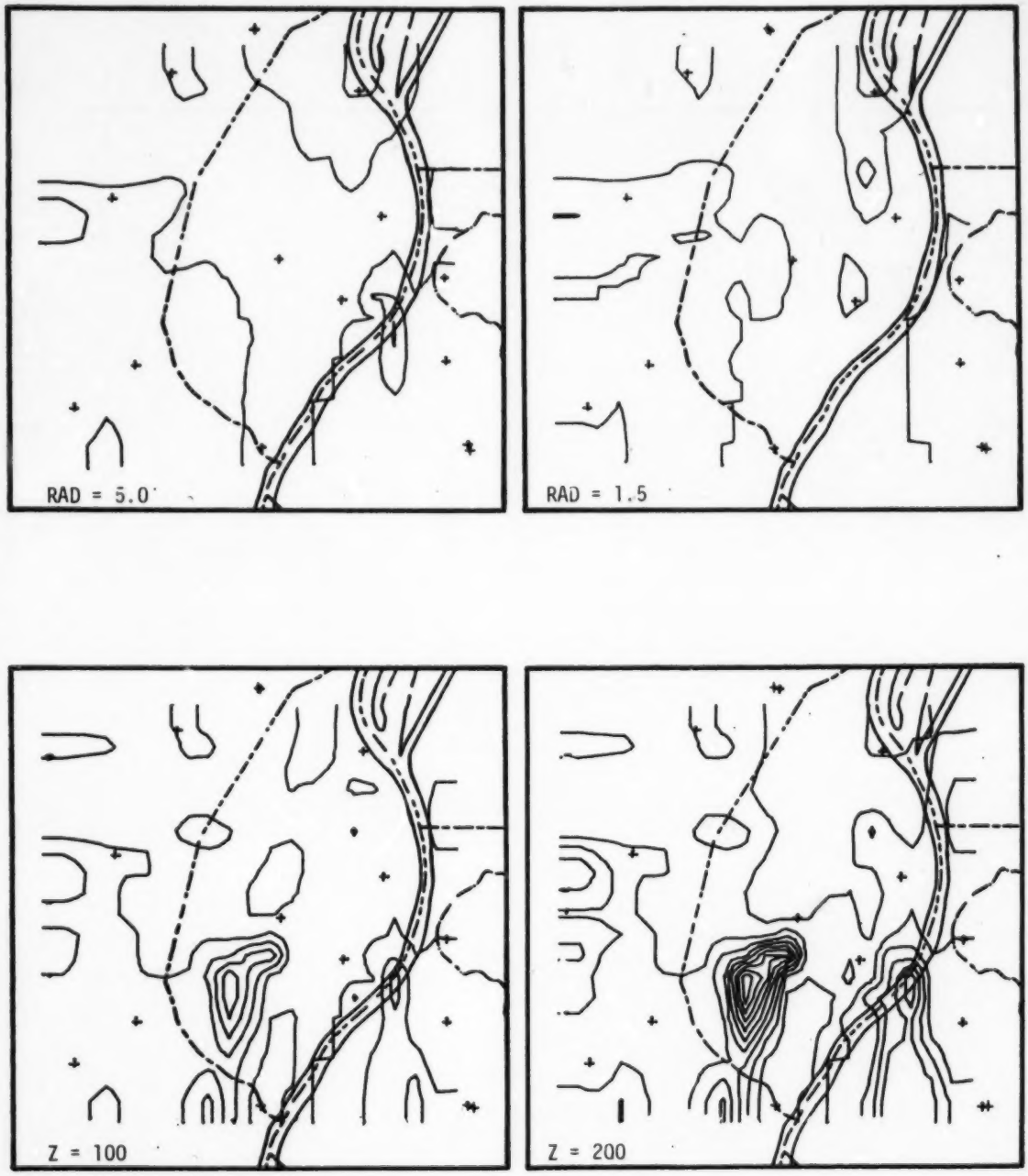

BEGIN LAST LINE OF TEXT
3/8"
OTTOM OF IMAGE AREA; OUTSIDE DIMENSION FOR TABLES AND ILLUSTRATIONS

Figure 7. (continued)

PAGE NUMBER
EPA-287 (Cin.)
(4-76)

BEGIN FIRST LINE OF TEXT HERE
TYPING GUIDE SHEET
CENTER OF PAGE
TOP OF IMAGE AREA
DROPPED HEAD; BEGIN SECTIONS HERE

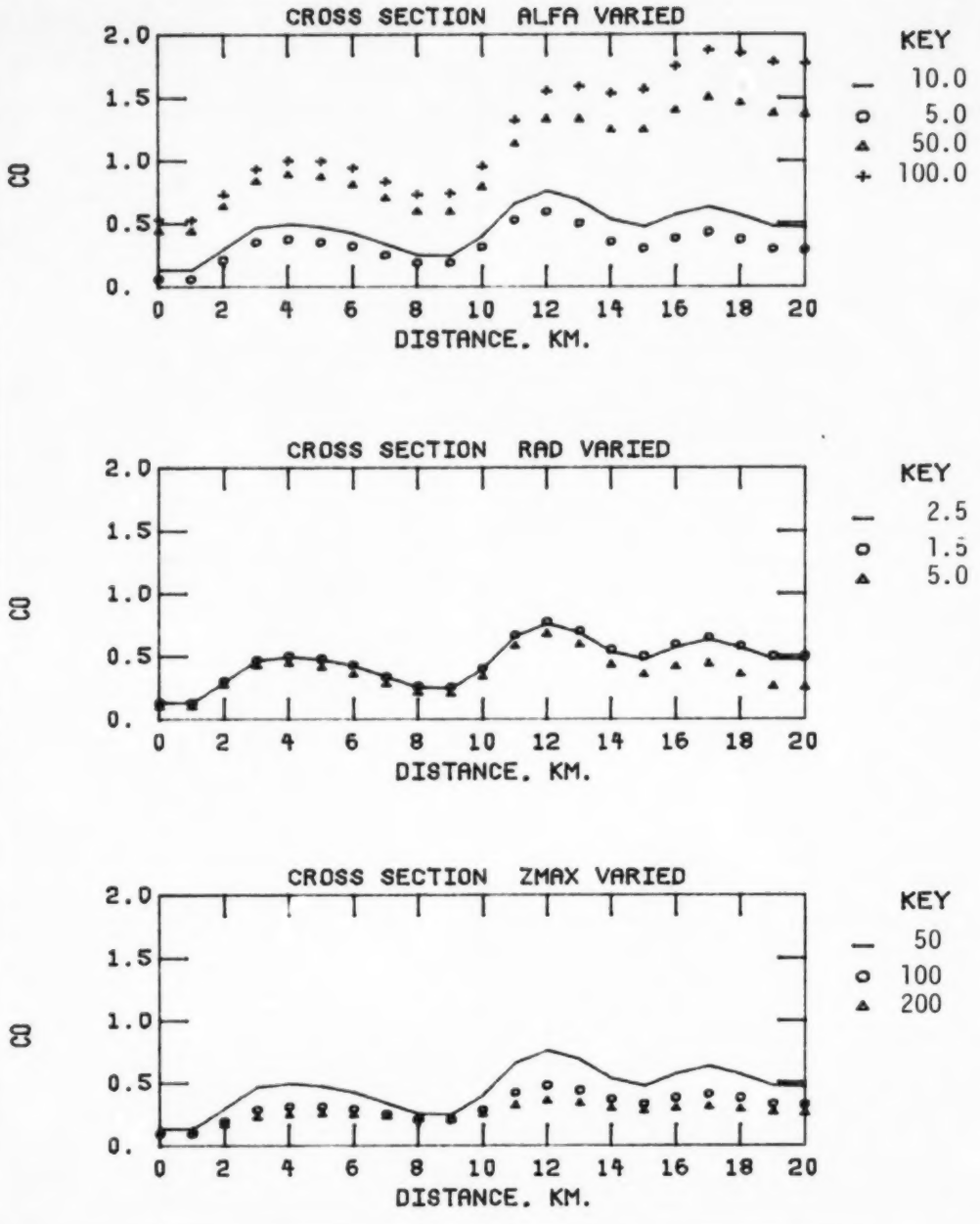

Figure 8. Spatial cross section of OVAM analysis (ppm) for sensitivity tests indicated in key.

BEGIN LAST LINE OF TEXT
BOTTOM OF IMAGE AREA, OUTSIDE DIMENSION FOR TABLES AND ILLUSTRATIONS
3/8"

EPA-287 (Cin.)
(4-76)

the Mississippi River downwind of the primary area sources (Figure 9). Concentration minima developed along the northwestern city limits and to the south-central portion of the city. To the southwest, RTI 205 did not report at 1100 CST, but data were available at 1200 CST, producing marked changes in the CO distribution in that area. The largest differences between the Barnes analysis and the OVAM analysis occurred near two network stations close to each other which are affected by major sources.

By 1300 and 1400 CST, the winds shifted to the south-southwest. The maximum associated with the emissions near the river shifted to a more north-south orientation, encroaching on the minimum in the south-central part of the city. The minimum in the northwest persisted. A maximum concentration just north of the center of the area developed because of a large area source just upwind of the maximum. In the previous two hours, the OVAM had been tempered by the observation at EPA 106, missing during these hours, and had attempted to increase the concentration at EPA 106, by 25 to 40 percent. Without the restriction of the observation, the relative weight of the analysis, / , locally decreases from 1.0 to 0.1 and favors the constraint equation.

At 1500 and 1600 CST, the winds were more southerly throughout the grid. An OSN station (STL 002) at the south-central location STL reported the largest CO concentration of any station. Furthermore, these were the only times this station reported during the eight-hour period. The large value dominates the analysis throughout the southwestern portion of the area. The area sources were inconsistent (smaller) with the observation in that area and did little to modify the impact of the initial interpolation. The influence of the observation did not extend to the east because of advective affects. Sources would have caused larger concentrations there thus making the maxima larger rather than smaller. Several streaks of higher concentration, downwind of sources were present. The maximum in the center of the area remained in about the same position at 1500 but was markedly reduced when EPA 106 reported data at 1600 CST.

From 1600 to 1700 CST, the concentration at EPA 120 more than doubled and dominated the analysis over the western half of the area. At other locations, the observations and OVAM concentrations showed small differences. Emissions had decreased markedly, especially along the river, thus, having less impact upon the analysis.

These analyses clearly show the influences of emissions and winds (the constraint equation) upon the resulting analyses. The 1500-1700 CST analyses clearly show that a large concentration observed in an area where the emissions does not justify such a large value, will dominate the analysis in that region. The area dominated is a function of the initial interpolation. The observation at EPA 120 at 1700 CST could be produced by sampling very close to a source though no major source is indicated in the emissions analysis. The large concentration at STL 002 at 1500 and 1600 CST was suggested by analyses at 1300 and 1400 CST. However, the magnitude of observed values at 1500 and 1600 CST, which are point observations, do not correspond to those of the emissions, which are area-averaged values. The discrepancy produced by employing point observations with area-averaged source

BEGIN FIRST LINE OF TEXT HERE
TYPING GUIDE SHEET
CENTER OF PAGE
TOP OF IMAGE AREA
DROPPED HEAD: BEGIN SECTION HERE

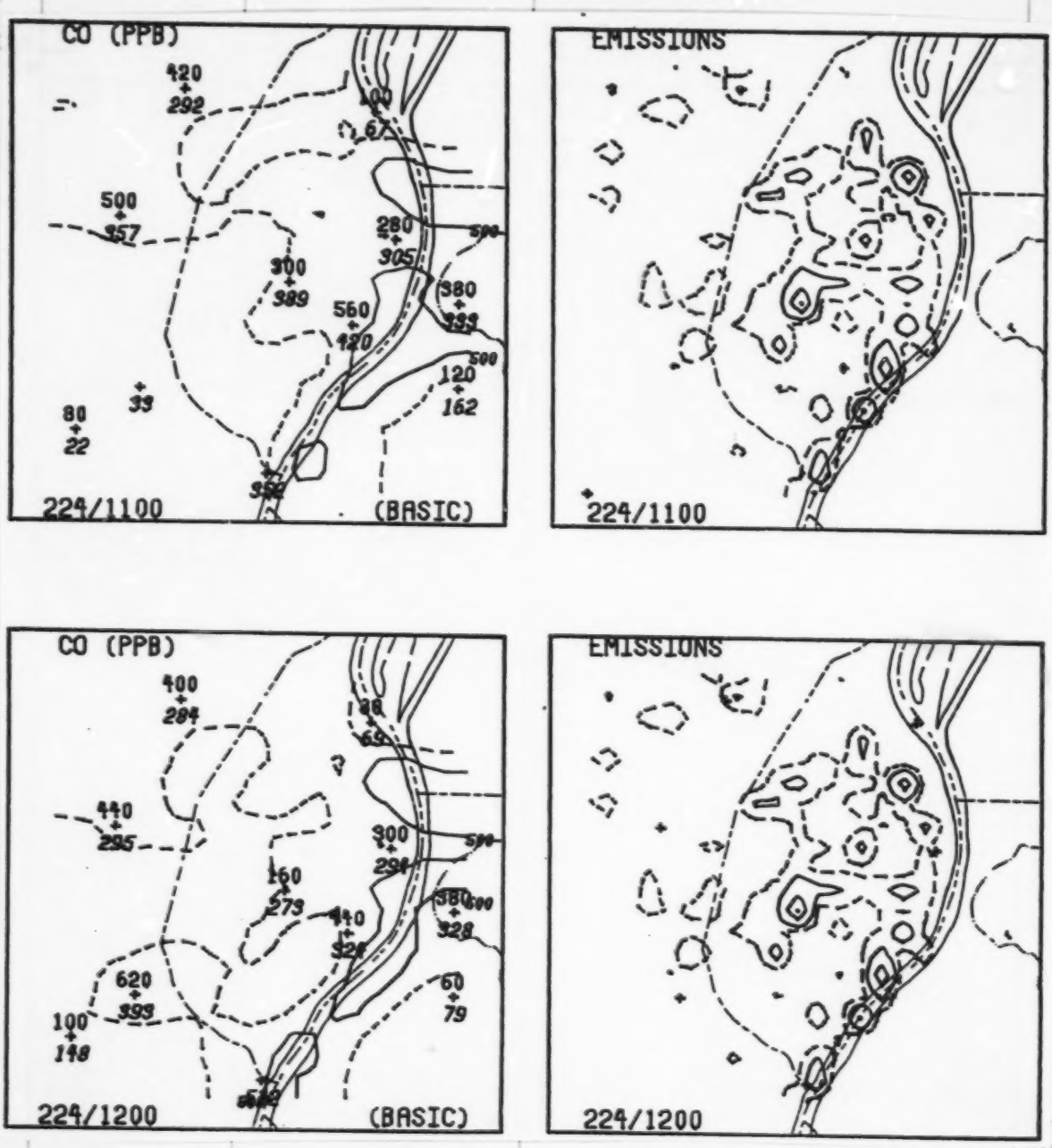

Figure 9. OVAM concentration analyses and area emissions by hour for August 12, 1975.

BEGIN LAST LINE OF TEXT
3/8"
BOTTOM OF IMAGE AREA; OUTSIDE DIMENSION FOR TABLES AND ILLUSTRATIONS

EPA-287 (Cin.)
(4-76)

BEGIN FIRST LINE OF TEXT HERE
TYPING GUIDE SHEET
CENTER OF PAGE
TOP OF IMAGE AREA
DROPPED HEAD: BEGIN SECTIONS HERE

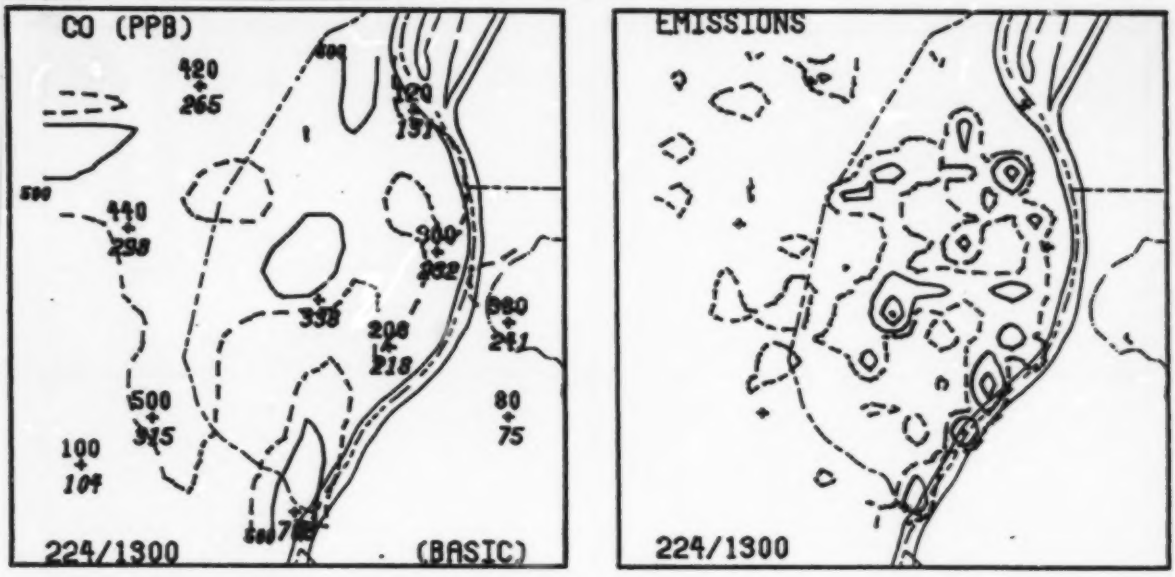

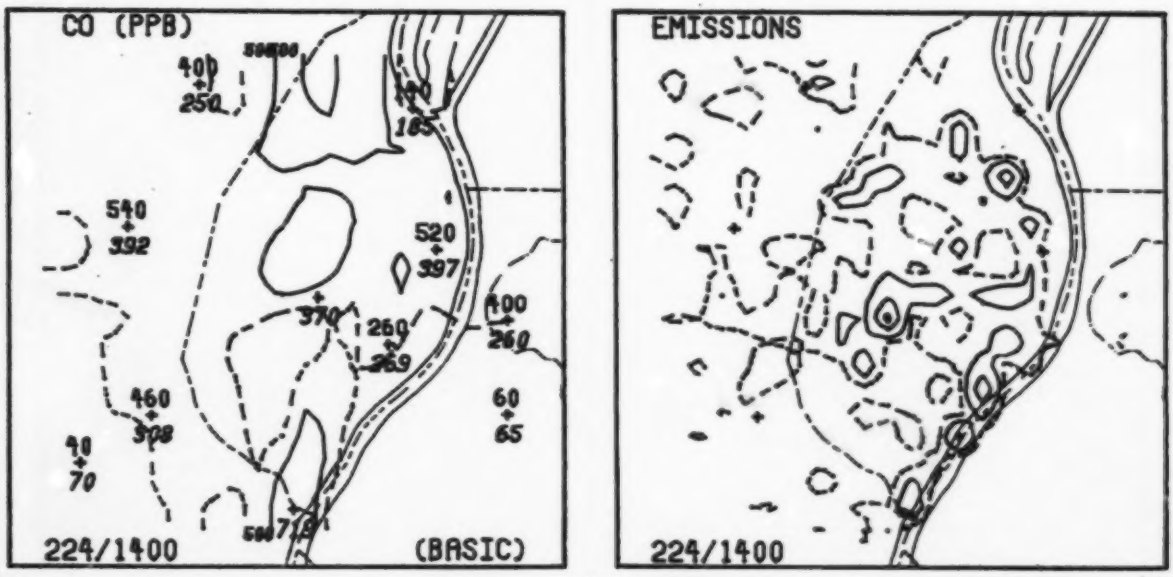

Figure 9. (continued)

BEGIN LAST LINE OF TEXT
BOTTOM OF IMAGE AREA. OUTSIDE DIMENSION FOR TABLES AND ILLUSTRATIONS
3/8"

EPA-287 (Cin.)
(4-76)

BEGIN FIRST LINE OF TEXT HERE
TYPING GUIDE SHEET
CENTER OF PAGE
TOP OF IMAGE AREA
DROPPED HEAD; BEGIN SECTIONS HERE

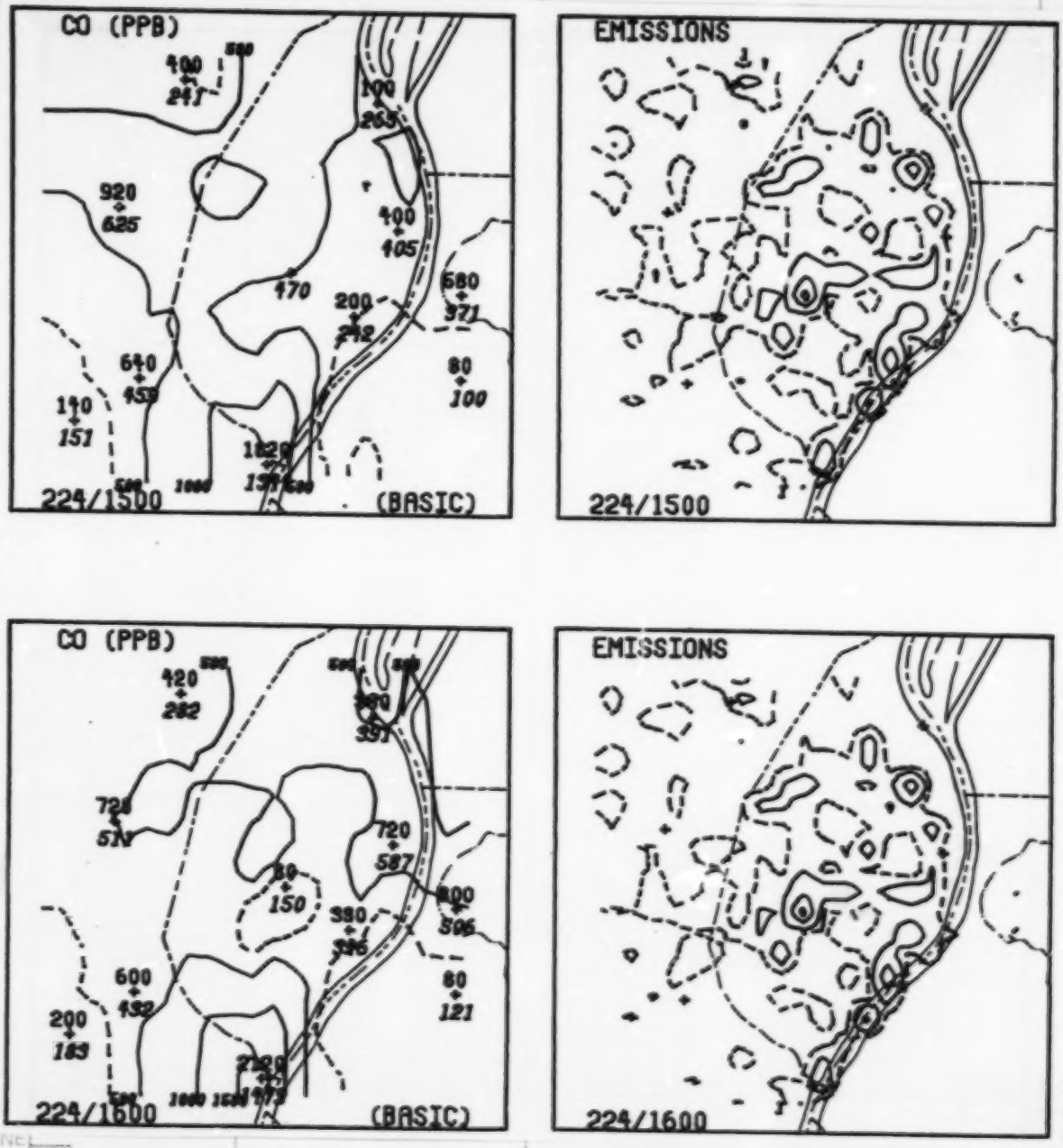

Figure 9. (continued)

BEGIN LAST LINE OF TEXT
BOTTOM OF IMAGE AREA; OUTSIDE DIMENSION FOR TABLES AND ILLUSTRATIONS
3/8"

EPA-287 (Cin.)
(4-76)

BEGIN FIRST LINE OF TEXT HERE
TYPING GUIDE SHEET
CENTER OF PAGE
TOP OF IMAGE AREA
DROPPED HEAD; BEGIN SECTIONS HERE

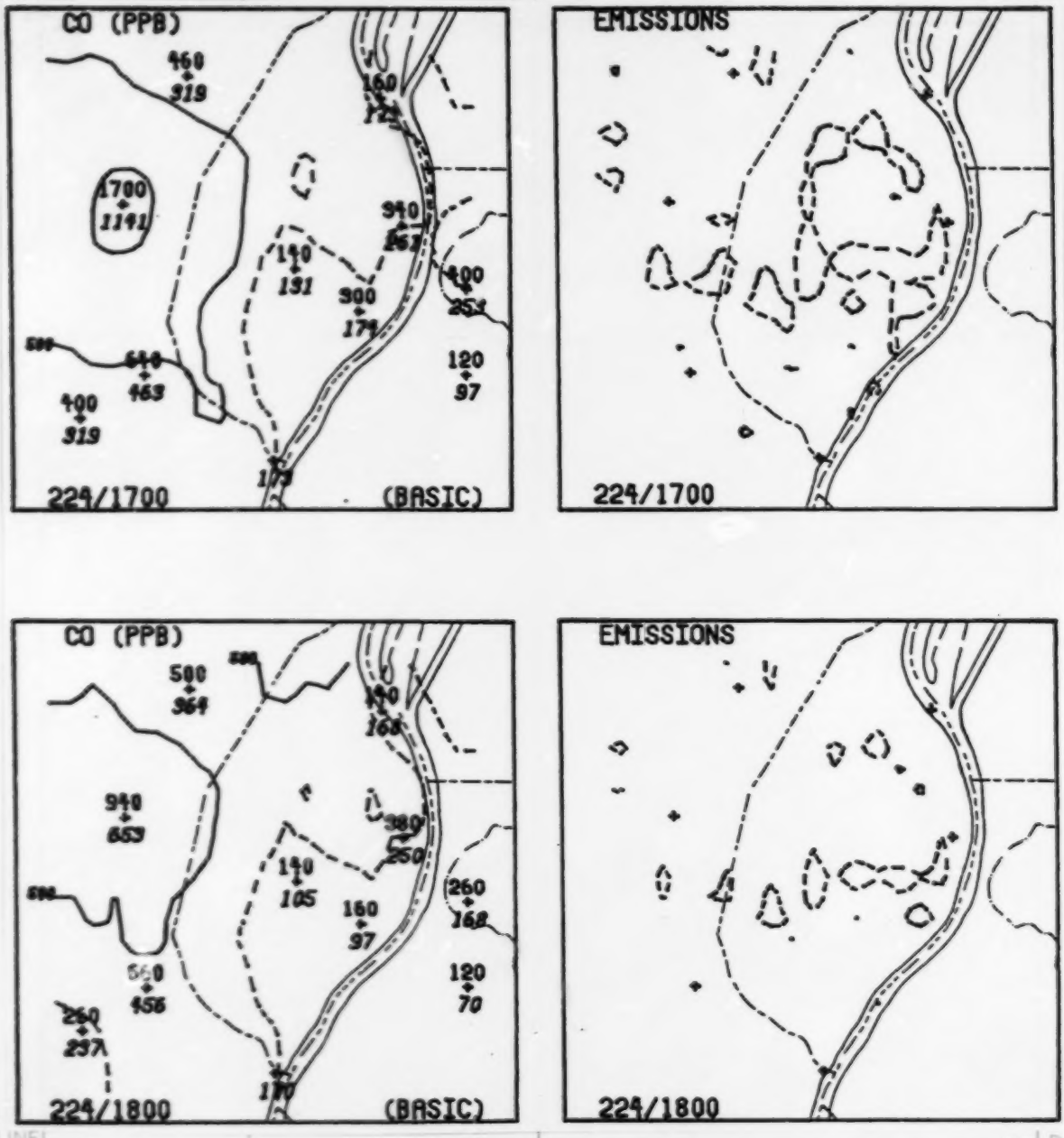

BEGIN LAST LINE OF TEXT
3/8"
BOTTOM OF IMAGE AREA, OUTSIDE DIMENSION FOR TABLES AND ILLUSTRATIONS

Figure 9. (continued)

EPA-287 (Cin.)
(4-76)

BEGIN FIRST LINE OF TEXT HERE
TYPING GUIDE SHEET
CENTER OF PAGE
TOP OF IMAGE AREA
DROPPED HEAD: BEGIN SECTIONS HERE

emissions is a significant problem that will always be encountered in utilizing an OVAM--or prediction models. The 1300 and 1400 CST analyses indicated that the large sources near STL 002 affected only a small area about the station, when the observation at that station was missing. The large area of influence demonstrated in the 1500 and 1600 CST analyses was due to the initial field created by the Barnes analysis.

The impact of the sources on the analyses appears significant. However, the concentrations are on the order of 0.5 ppm. The largest hourly concentration is on the order of 2 ppm or about one-fourth the NAAQS for eight-hour running averages for CO. The case study treats CO concentrations which are near the measurement capability of the instrument used to measure CO. A comparison of observed and interpolated concentrations nearest the observing locations is given in Table 2.

DELETION OF OBSERVATIONS

The summer case study was primarily chosen to examine the effects of missing observations. This analysis was carried out by randomly deleting observations from the set of available observations for a given hour. The selection procedure was random so that user bias would not be an influence. It also needed to be repeatable from analysis to analysis. The number of OSN observations to be deleted and an initial number for the random number generator are input parameters for the selection procedure. The random number generator develops a number between 1 and the total number of OSN stations. If that observation is not missing or already deleted, it becomes a missing observation. The procedure repeats until the prescribed number of observations are deleted. The Barnes analyses are rerun on these revised data bases; the Barnes analysis is used to initialize the OVAM. In this manner, the whole analysis procedure is compared, not just the OVAM procedure. The status of the OSN stations in the various analyses is given in Table 3.

The OVAM value at the grid point nearest two non-network stations (EPA 107 and EPA 111) were plotted versus time (Figure 10). Concentrations at two OSN network locations were similarly identified. One of those stations (EPA 105) had CO observations for the entire period; the other (EPA 106) did not report from 1300 to 1500 CST.

Station EPA 105 was deleted from all hours when six data points were removed and from the 1300 to 1500 CST when two data points were removed. When the data were retained, the OVAM value at the nearest grid point and the observed value at the point are in good agreement. When the observations were removed, the OVAM overpredicts, especially when station EPA 106 is also missing. EPA 105 was downwind of large area sources (Figure 9). The discrepancy between observation and prediction suggests either the emissions were too large or the observations were too small.

Station EPA 106 was not used in the analyses when two stations were removed and at 1600 CST when six stations were removed. When the data were not missing or removed, the OVAM showed reasonable agreement with the observation. The substantial difference in the OVAM and the observations in other cases was a result of the station's proximity to the large area source,

BEGIN LAST LINE OF TEXT
BOTTOM OF IMAGE AREA, OUTSIDE DIMENSION FOR TABLES AND ILLUSTRATIONS
3/8"

EPA-287 (Cin.)
(4-76)

TABLE 2. CO CONCENTRATIONS (ppb) OBSERVED AND INTERPOLATED BY THE BARNES AND OVAM FOR OSN STATIONS WITHIN THE ANALYSIS GRID (AUGUST 12, 1975)

Station	1100			1300			1500			1700		
	OBS	Barnes	OVAM	OBS	Barnes	OVAM	OBS	Barnes	OVAM	OBS	Barnes	OVAM
RTI 202	420	423	416	420	369	426	400	409	406	460	479	461
STL 009	500	501	489	440	383	411	920	921	833	1,700	1,723	1,632
RTI 205	M	54	137	500	381	403	640	552	548	640	616	603
STL 002	M	179	361	M	375	755	1,820	1,809	1,843	M	453	478
EPA 101	280	295	318	300	257	320	400	384	492	340	328	332
EPA 102	100	107	144	120	107	208	100	109	356	160	176	279
EPA 104	380	365	427	380	304	326	580	515	480	400	376	330
EPA 105	560	498	447	200	181	327	200	221	378	300	263	244
EPA 106	300	320	369	M	207	569	M	265	714	140	174	162
EPA 110	120	165	221	80	100	122	80	141	165	120	155	136
EPA 119	80	80	38	100	111	115	140	156	147	400	415	390

M = missing observation

BEGIN LAST LINE OF TEXT
EPA-287 (Cin.) (4-76)
3/8"
PAGE NUMBER
37
AND ILLUSTRATIONS
BOTTOM OF IMAGE AREA. OUTSIDE DIMENSION FOR TABLES
9 1/8"
6 1/2"
DROPPED HEAD. BEGIN SECTIONS HERE
BEGIN FIRST LINE OF TEXT HERE
TYPING GUIDE SHEET
CENTER OF PAGE
TOP OF IMAGE AREA

BEGIN FIRST LINE OF TEXT HERE
TYPING GUIDE SHEET
CENTER OF PAGE
TOP OF IMAGE AREA
DROPPED HEAD; BEGIN SECTIONS HERE

TABLE 3. MISSING AND DELETED OBSERVATIONS (August 12, 1975)

Station	1100	1200	1300	1400	1500	1600	1700	1800
STL 008	M	M	M	M	M	M	M	M
RTI 202	4	4	4	4	4	4	4	4
STL 009	2,4	2,4	2,4	2,4	2,4	2,4	2,4	2,4
STL 006	M	M	M	M	M	M	M	M
RTI 205	M	4,6	4,6	4,6	4,6	4,6	4,6	4,6
STL 002	M	M	M	M	6	6	M	M
RTI 207	M	M	M	M	M	M	M	M
EPA 101	6	6	6	6	6	6	6	6
EPA 102	6	6	6	6	6	6	6	6
EPA 104	6	---	6	6	---	---	---	---
EPA 105	6	6	2 6	2 6	2 6	6	6	6
EPA 106	2 6	2 6	M	M	M	2	2 6	2 6
EPA 108	---	---	---	---	---	---	---	---
EPA 109	---	---	M	M	M	M	M	---
EPA 110	4,6	4,6	4,6	4,6	4,6	4,6	4,6	4,6
EPA 113	4	---	---	---	---	---	---	---
EPA 118	---	---	---	---	---	---	---	---
EPA 119	---	---	---	---	---	---	---	---
EPA 120	---	---	---	---	---	---	---	---

2 - deleted, one of two
4 - deleted, one of four
6 - deleted, one of six
M - missing observation

suggesting, as in the case of EPA 105, that the emissions were too large or the observations were too small.

At the non-network stations (EPA 107 and 111), the OVAM value does not generally follow the trends of the observed concentration. However, the observed concentrations are so small that differences with analyses are not necessarily meaningful. The presence or absence of data does not usually affect the concentration estimates. However, the concentrations at EPA 111 at 1500 CST results from a complex interaction of sources, observations, and deleted observations. The best estimate occurs with six stations missing, the poorest with two. This station is just downwind from the large area source and the reported large concentration at STL 002. With EPA 105 (and one other

BEGIN LAST LINE OF TEXT
BOTTOM OF IMAGE AREA, OUTSIDE DIMENSION FOR TABLES AND ILLUSTRATIONS
3/8"

EPA-287 (Cin.)
(4-76)

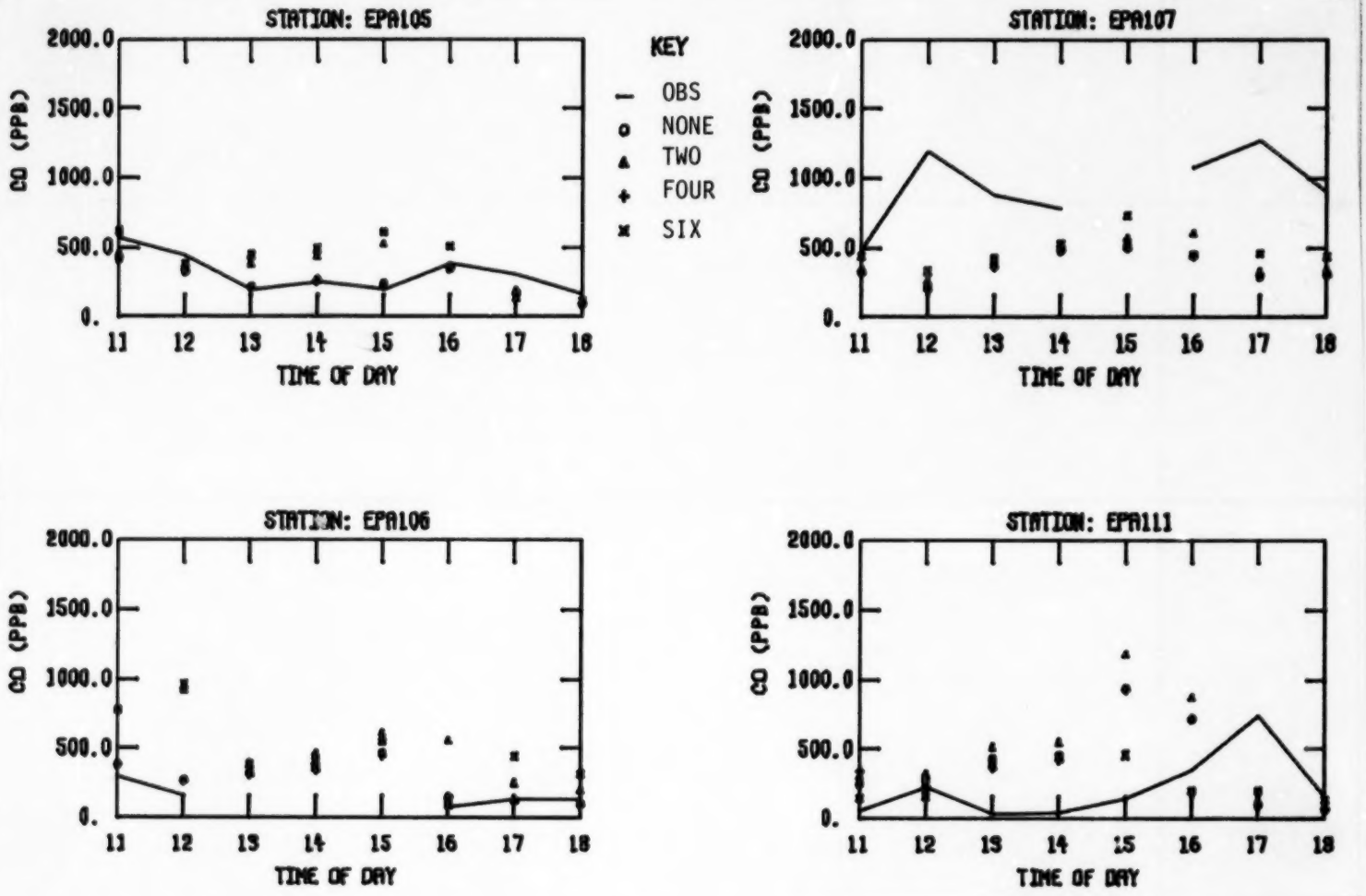

Figure 10. Time series of observed and interpolated CO concentrations for indicated number of missing observations for August 12. Stations to left were in OSN; those to right were not.

BEGIN LAST LINE OF TEXT
DROPPED HEAD: BEGIN SECTIONS HERE
BEGIN FIRST LINE OF TEXT HERE
TYPING GUIDE SHEET
EPA-287 (Cin.) (4-76)
3/8"
PAGE NUMBER
39
CENTER OF PAGE
BOTTOM OF IMAGE AREA, OUTSIDE DIMENSION FOR TABLES AND ILLUSTRATIONS
TOP OF IMAGE AREA

BEGIN FIRST LINE OF TEXT HERE
TYPING GUIDE SHEET
CENTER OF PAGE
TOP OF IMAGE AREA
DROPPED HEAD; BEGIN SECTIONS HERE
6-1/2"
BEGIN LAST LINE OF TEXT
3/8"
BOTTOM OF IMAGE AREA; OUTSIDE DIMENSION FOR TABLES AND ILLUSTRATIONS
PAGE NUMBER
EPA-287 (Cln.) (4-76)

station) deleted and EPA 106 missing, the concentration at EPA 111 is dominated by the large concentration at STL 002. However, when six stations are deleted, STL 002 is also deleted, so the OVAM estimate is more consistent with those at the earlier hours.

The consequences of deleting measurements upon the spatial distribution of CO produced by the OVAM are shown in Figure 11. For each hour, the isopleths of CO for the basic case and the spatial distribution of the percentage change of concentration as a result of removing two, four, and six observations from those available are shown. The removed observations are indicated by a large dot in each frame of the figure.

The random selection process produced a diverse set of data deletions. When four observations are deleted, three of the four stations are in the western extremity of the analysis region, and one is on the southeast border. For most of the hours, only one observation (EPA 119) remains in the southern and western third of the analysis area. The same six stations are not deleted each time, but five are in the eastern half of the area, often being adjacent to the river and sources. One southwestern station is deleted.

The impact of removing an observation depends upon the wind direction. When the winds were westerly (1100 and 1200 CST), a large percentage increase occurred near EPA 102 along the axis of the wind when the observation from that station was deleted (one of six stations only). As the winds turned southerly (1300 to 1600 CST), the axis of the increase became oriented south to north. The changes around EPA 106 (two stations removed) at 1100, 1200, and 1600 CST show the same rotation of axes.

The removal of the three western stations invariably produced a one-half to three-fourths reduction in the OVAM predictions through the western half of the domain. The reduction is attributable to reduced concentration estimates for the Barnes analysis and the fact that no large sources are found in the immediate vicinity. The deletion of those data tended to reduce the concentration slightly in the eastern portion of the area, (except to the southeast of the river) regardless of the wind direction.

To the southeast of the Mississippi River in an area almost devoid of sources, the removal of the observation at EPA 110 has a dramatic impact upon the concentrations that persist through all analyses. The concentrations in that area are controlled by the background concentrations (i.e., the minimum concentration permitted in the analysis). For the four- and six-station deleted analyses, the background concentrations were two to five times the background of the basic case, particularly upwind of EPA 106.

Almost all analyses show a major percentage increase from the basic case when EPA 106, the most central station, is removed from the analysis. The OVAM analysis increased the concentration near EPA 106 in response to the nearby source. When the station value is missing or deleted, the increases are not constrained as when the data are present.

The 27 February 1976 case was also used to examine some effects of missing observations. The deletion of six observations from the OVAM network

BEGIN FIRST LINE OF TEXT HERE
TYPING GUIDE SHEET
CENTER OF PAGE
TOP OF IMAGE AREA
DROPPED HEAD: BEGIN SECTION HERE

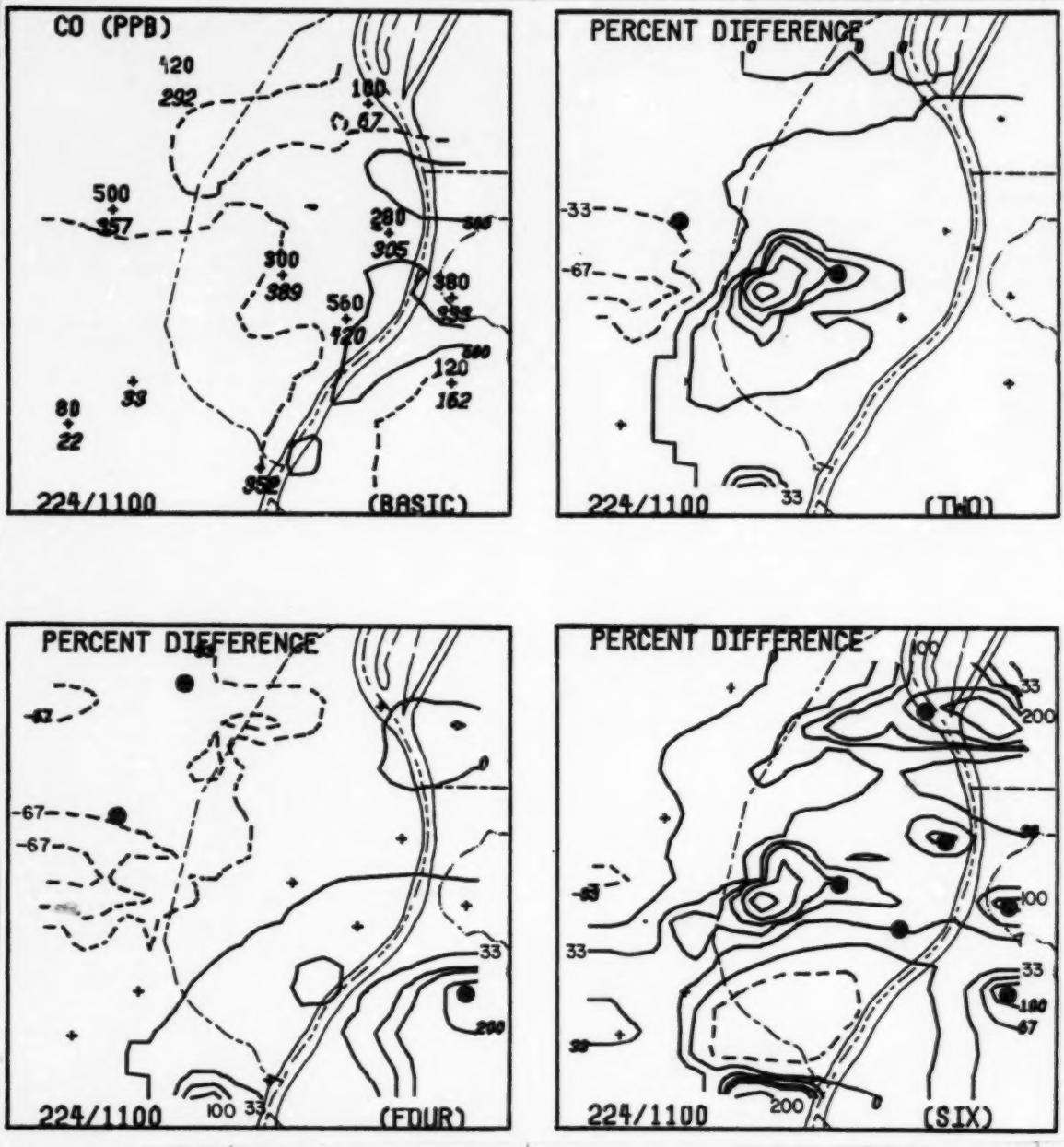

Figure 11. Isopleths of concentration for basic case and percent change with two, four or six stations deleted, August 12, 1975. Deleted stations are indicated (•). Isopleths of percent change are -67, -33, 0, 33, 67, 100, 200, and 400.

BEGIN LAST LINE OF TEXT
BOTTOM OF IMAGE AREA, OUTSIDE DIMENSION FOR TABLES AND ILLUSTRATIONS
3/8"

EPA-287 (Cin.)
(4-76)

BEGIN FIRST LINE OF TEXT HERE
TYPING GUIDE SHEET
CENTER OF PAGE
TOP OF IMAGE AREA
DROPPED HEAD; BEGIN SECTIONS HERE

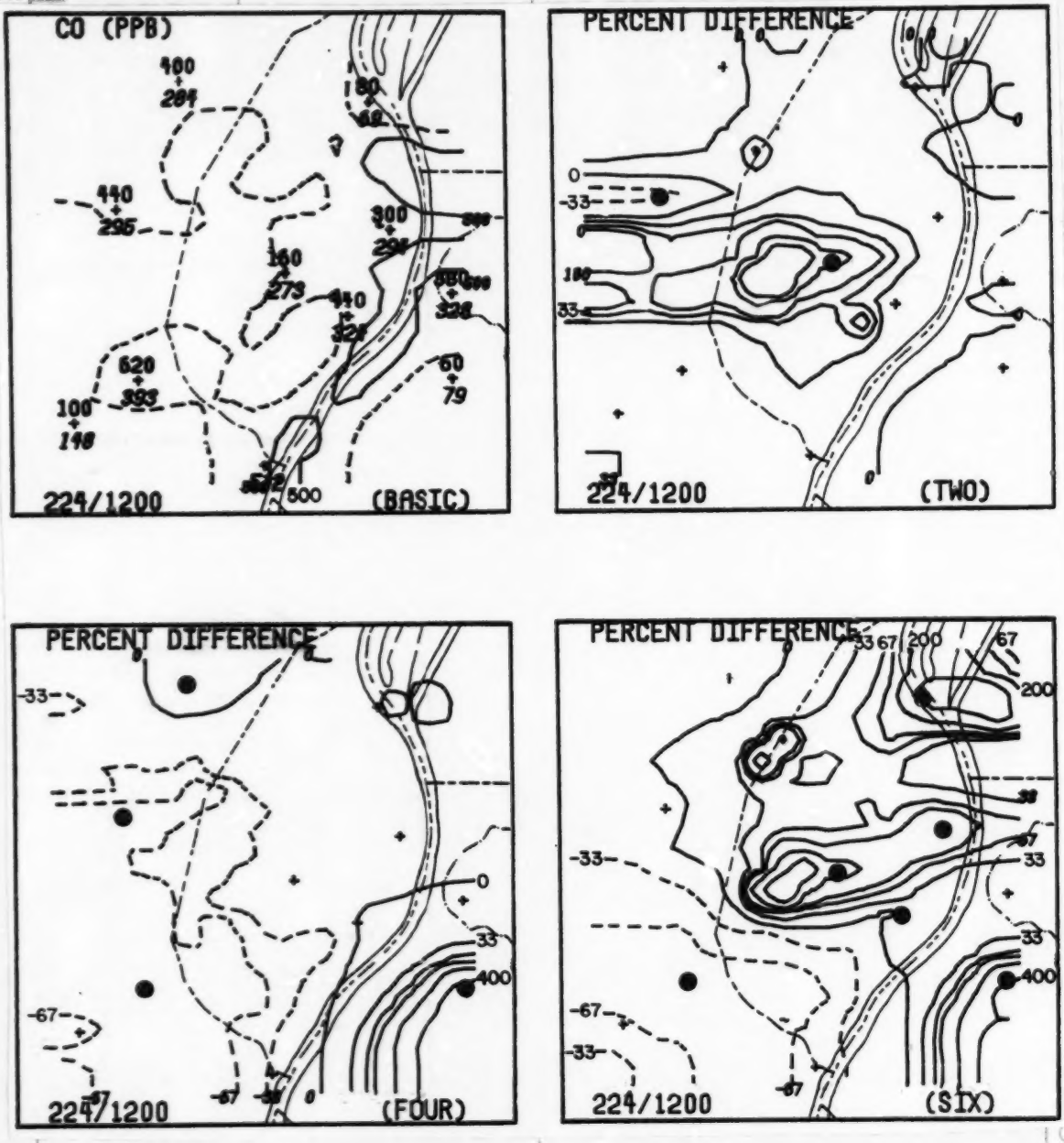

Figure 11. (continued)

BEGIN LAST LINE OF TEXT
3/8"
BOTTOM OF IMAGE AREA; OUTSIDE DIMENSION FOR TABLES AND ILLUSTRATIONS

EPA-287 (Cin.)
(4-76)

BEGIN FIRST LINE OF TEXT HERE
TYPING GUIDE SHEET
CENTER OF PAGE
TOP OF IMAGE AREA
DROPPED HEAD; BEGIN SECTIONS HERE

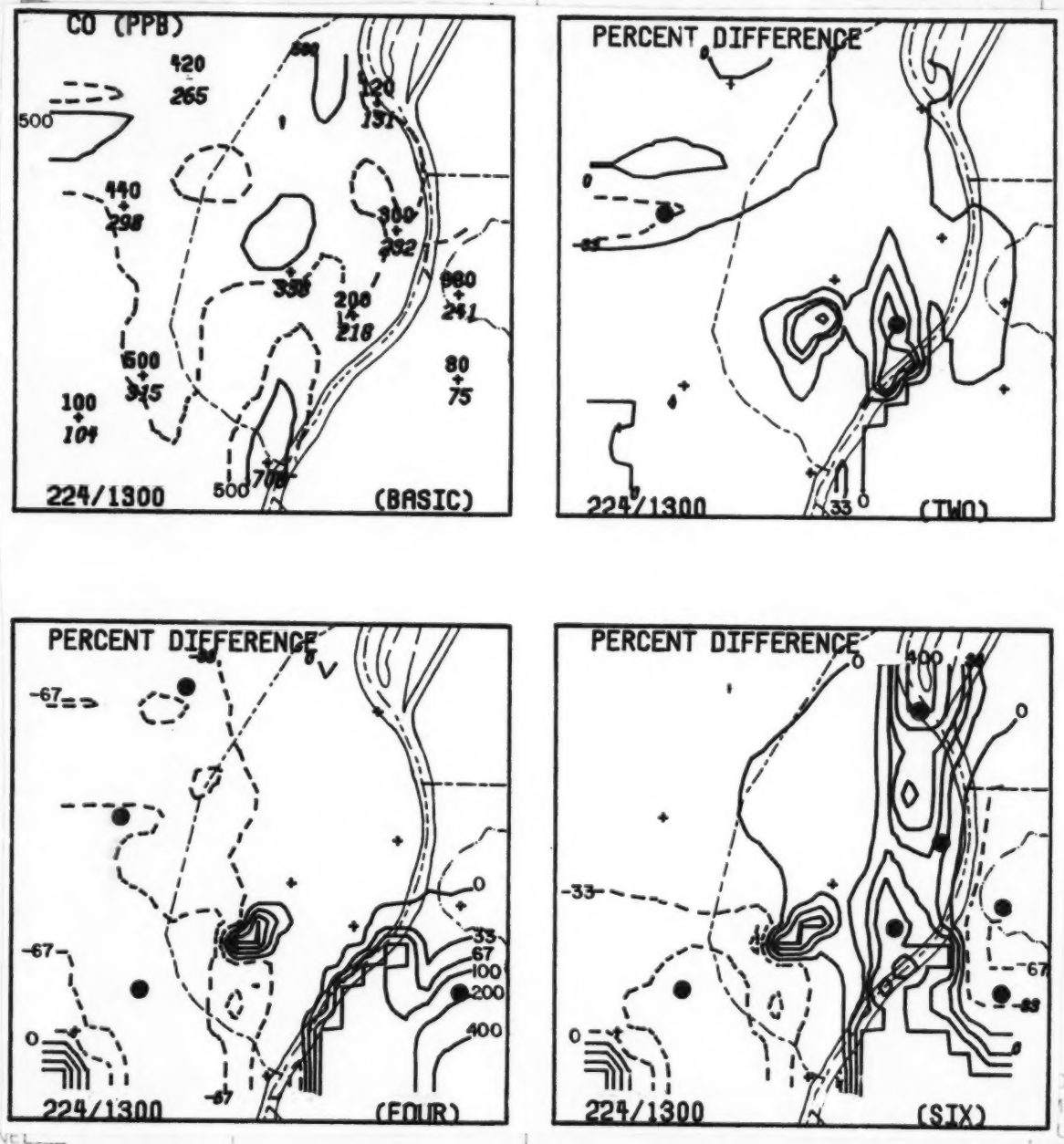

BEGIN LAST LINE OF TEXT
BOTTOM OF IMAGE AREA; OUTSIDE DIMENSION FOR TABLES AND ILLUSTRATIONS
3/8"

Figure 11. (continued)

EPA-287 (Cin.)
(4-76)

BEGIN FIRST LINE OF TEXT HERE
TYPING GUIDE SHEET
CENTER OF PAGE
TOP OF IMAGE AREA
DROPPED HEAD; BEGIN SECTION HERE

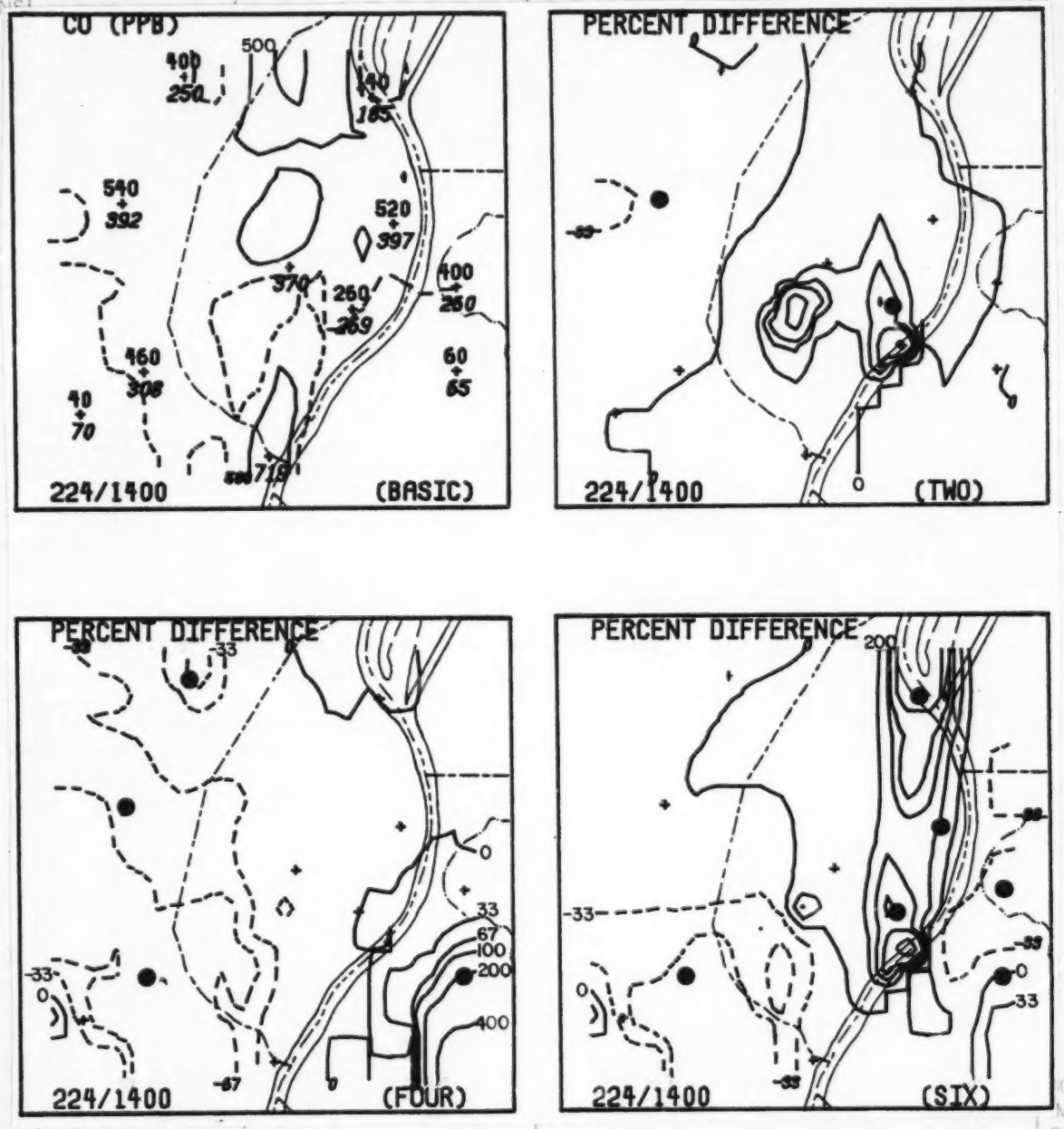

Figure 11. (continued)

BEGIN LAST LINE OF TEXT
BOTTOM OF IMAGE AREA; OUTSIDE DIMENSION FOR TABLES AND ILLUSTRATIONS
3/8"

EPA-287 (Cin.)
(4-76)

BEGIN FIRST LINE OF TEXT HERE
TYPING GUIDE SHEET
CENTER OF PAGE
TOP OF IMAGE AREA
DROPPED HEAD; BEGIN SECTIONS HERE

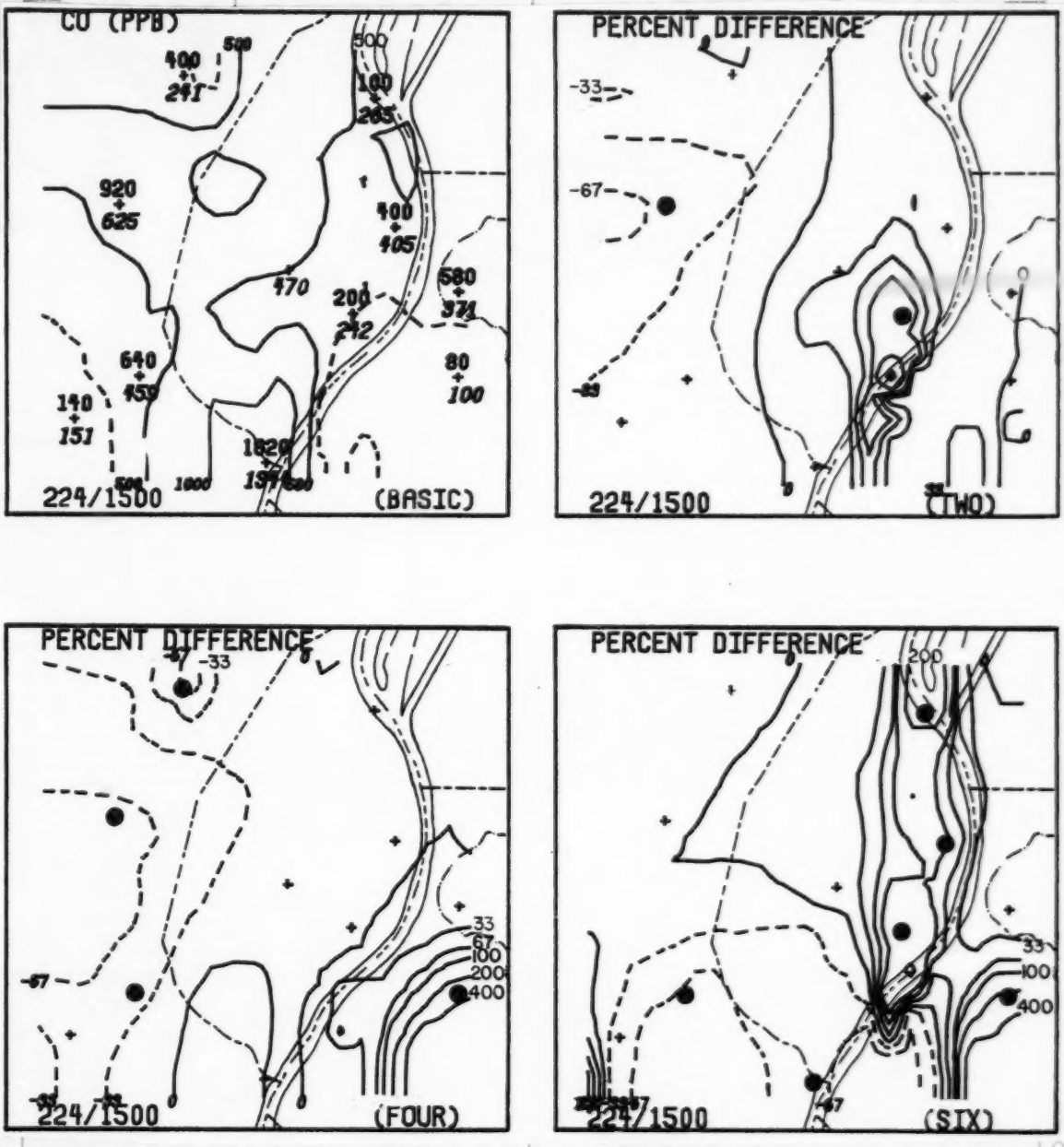

BEGIN LAST LINE OF TEXT
BOTTOM OF IMAGE AREA; OUTSIDE DIMENSION FOR TABLES AND ILLUSTRATIONS
3/8"

Figure 11. (continued)

EPA-287 (Cin.)
(4-76)

BEGIN FIRST LINE OF TEXT HERE
TYPING GUIDE SHEET
CENTER OF PAGE
TOP OF IMAGE AREA
DROPPED HEAD: BEGIN SECTIONS HERE

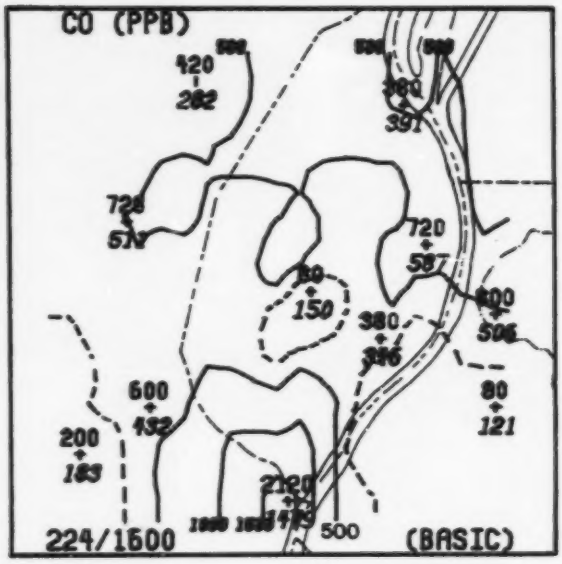

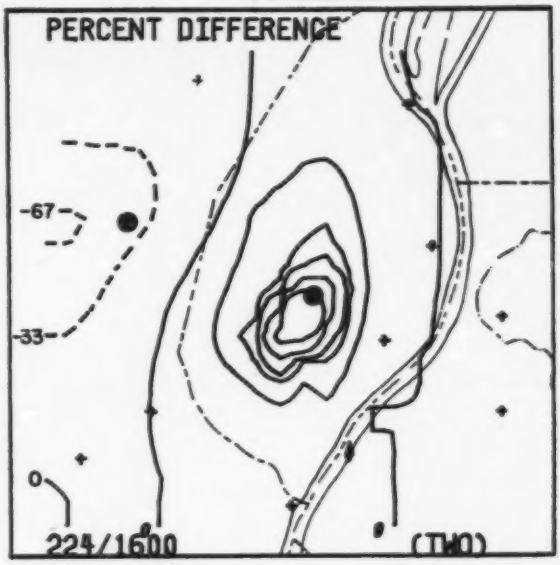

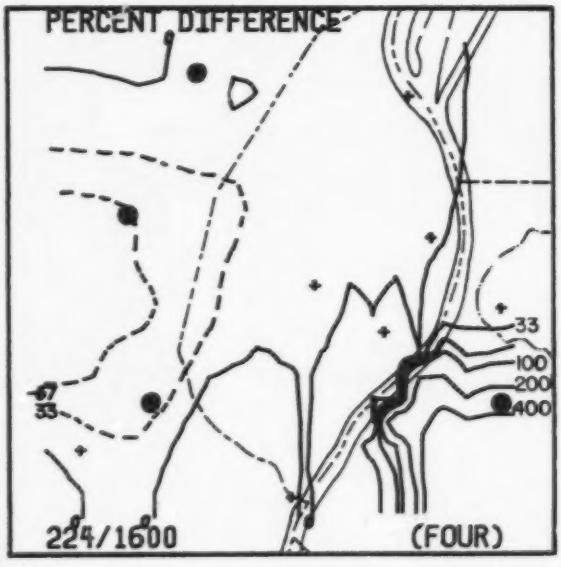

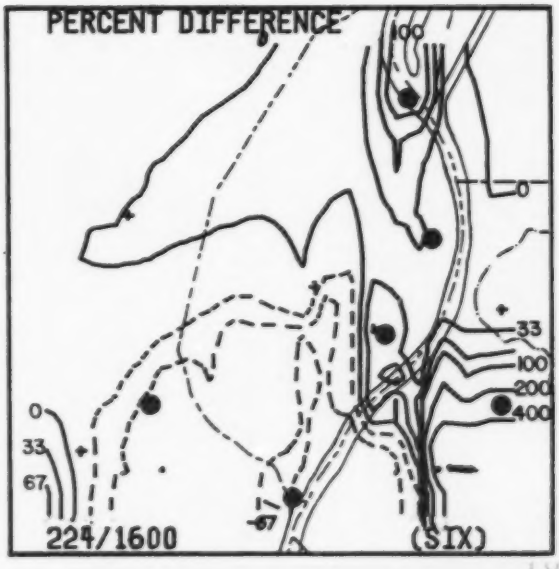

Figure 11. (continued)

BEGIN LAST LINE OF TEXT
3/8"
BOTTOM OF IMAGE AREA: OUTSIDE DIMENSION FOR TABLES AND ILLUSTRATIONS

EPA-287 (Cin.)
(4-76)

during the early morning of 27 February, produced substantial percentage changes of the analysis (Figure 12). Between 0000 to 0800 CST, the same five stations (STL 008, EPA 110, STL 002, EPA 105 and EPA 101) were deleted. For the first four hours, EPA 106 was deleted; and for the remaining hours, RTI 205 was deleted.

Throughout the night, station EPA 109 reported the highest concentrations of any station and dominated the analysis over a wide region. For the first four hours, the largest change occurred in the locality of EPA 106, a deleted station. Adjacent stations EPA 101 and EPA 105 were also deleted, leaving a void in the center of the grid. The initial interpolation in those areas was controlled by OSN stations giving higher concentrations than observed. At night, area sources diminished by an order of magnitude over daytime values, so that the emissions were too small, once again signalling a disparity between emissions and observed concentrations. Solutions were achieved in a few iterations. Local percent changes from the Barnes analysis to the OVAM analysis were generally less than $\pm$ 25 percent. Changes arose from changes in the initial conditions, rather than from the requirements of the constraint equation.

Comparison of observed concentration with OVAM predictions prior to 0600 CST suggest reasonable agreement (Figure 13). The OSN stations, EPA 106 and EPA 105, maintain reasonable agreement with the observations during this period. At 0700 and 0800 CST, when the observations at EPA 107, EPA 111 and EPA 106 increase five fold, that at EPA 105 remains about the same. The OVAM values, however, show an increase at EPA 105 of about five fold. The response of the OVAM to the high initial values and to the overall increase in emissions are probably responsible for this increase.

The concentration estimates for non-network stations, EPA 107 and EPA 111, show trends similar to the observed values. However, differences between predictions and observations for the non-network stations are generally greater than those for the network stations, especially between 0600 and 0800 CST. The observations at only EPA 107 are better predicted when six stations are missing. Also, the OVAM values generally differ little from the initial Barnes values, at both non-network and network stations.

EFFECTS OF BOUNDARY CONDITIONS ON ANALYSES

The OVAM predictions obtained with six stations withheld from the Barnes analysis were examined at OSN and non-network stations to determine error reduction and the number of iterations required to attain a solution for two sets of boundary conditions, the open boundary condition and $\delta \left(\frac{\partial \psi}{\partial n}\right) = 0$. For the August case study, the mean difference between the two sets of analyses was less than 60 ppb for all hours. The integrated error variance associated with the two solutions differed by less than two percent for each hour. The number of iterations occasionally varied but only because convergence had not occurred in less than [illegible] iterations in one analysis and did occur in others. However, a steady state of error reduction was attained in almost the same number of iterations. Thus, the boundary conditions did not have a major impact upon the results obtained.

BEGIN FIRST LINE OF TEXT HERE
TYPING GUIDE SHEET
CENTER OF PAGE
TOP OF IMAGE AREA
DROPPED HEAD: BEGIN SECTIO HERE

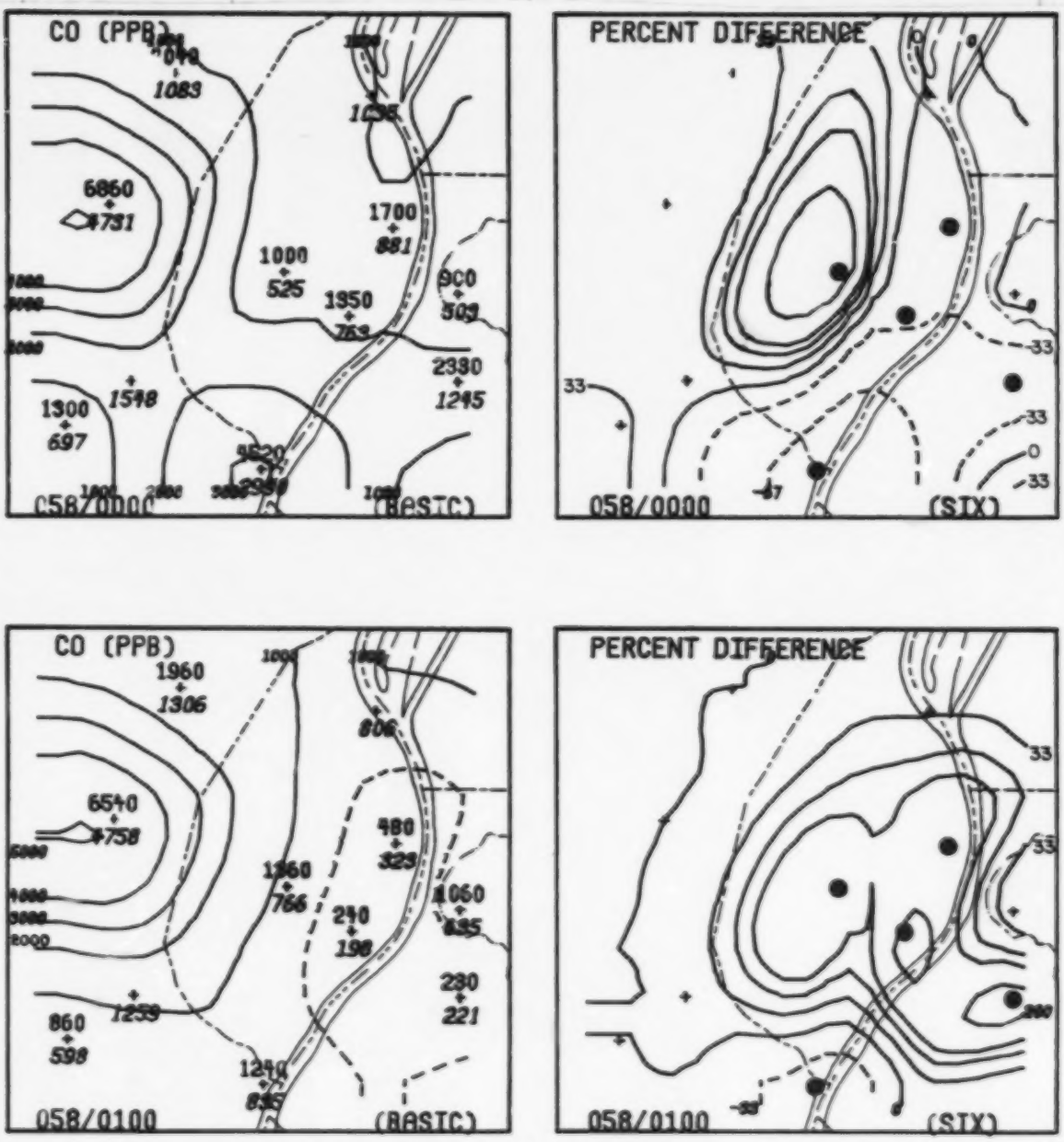

Figure 12. Isopleths of concentration for basic case and percent change with two, four, or six stations deleted, February 27, 1976. Deleted stations are indicated (•).

BEGIN LAST LINE OF TEXT
BOTTOM OF IMAGE AREA; OUTSIDE DIMENSION FOR TABLES AND ILLUSTRATIONS
3/8"

PAGE NUMBER
EPA-287 (Cin.)
(4-76)

BEGIN FIRST LINE OF TEXT HERE
TYPING GUIDE SHEET
CENTER OF PAGE
TOP OF IMAGE AREA
DROPPED HEAD. BEGIN SECTION HERE

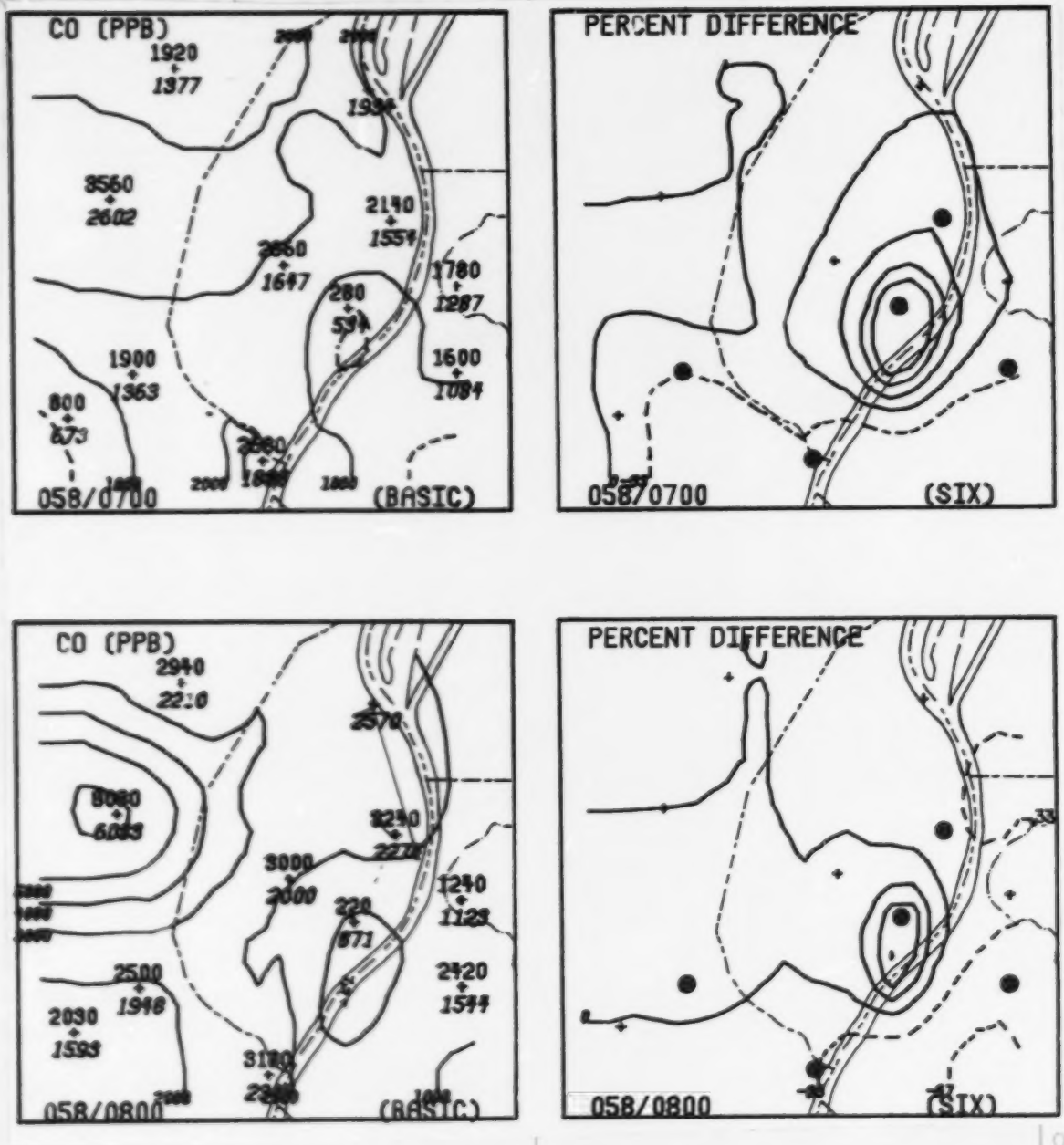

Figure 12. (continued)

BOTTOM OF IMAGE AREA. OUTSIDE DIMENSION FOR TABLES AND ILLUSTRATIONS
BEGIN LAST LINE OF TEXT
3/8"

EPA-287 (Cin.)
(4-76)

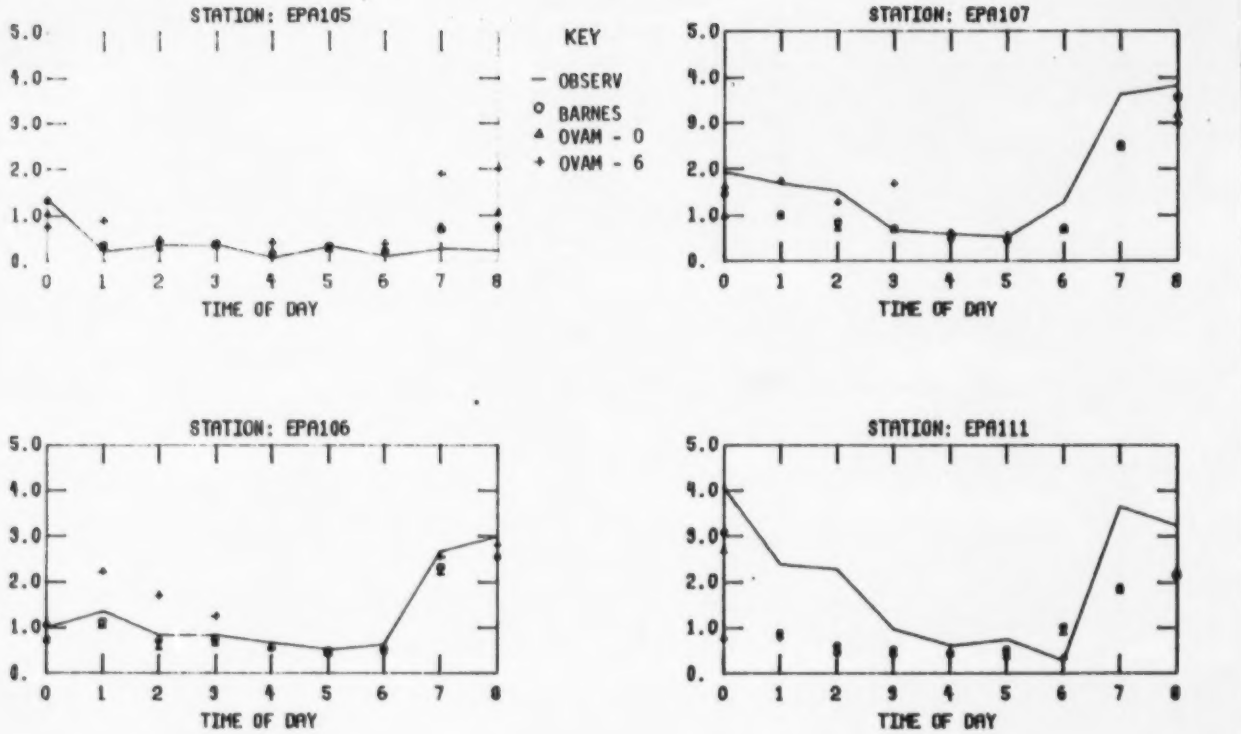

Figure 13. Time series of CO concentrations (ppm) for OSN and non-OSN locations from observations, Barnes interpolation and OVAM analysis with zero or six stations missing, February 27, 1976.

ERROR VARIANCE

The OVAM is designed to reduce the integrated error variance (EV) of the analysis over an area. In VBC, the EV was reduced to one-tenth of its initial value where the initial value was determined from an inverse square interpolation of randomly located, but analytically determined, "observations". The integrated EV of the Barnes and OVAM analysis are given in Table 4. The values were computed from the non-dimensional values with background subtracted. The daytime analyses show the largest variance with both the Barnes and the OVAM analyses. The EV increases through the day to a peak, then decreases rapidly as emissions diminish toward evening. Typically, the EV is reduced to about 78 percent of its initial value.

Removing observations from the input to the analyses has different effects upon the initial variance and its reduction by the OVAM. Removing two observations usually leads to a larger initial and final EV. When four observations are removed the initial EV is reduced. An exception occurred at 1500 and 1600 CST in August, 1975 and the initial error variance increased when the large concentration at STL 002 was reported. The interpolated values in the western third were lower and more in keeping with the lower emissions in the areas (Figure 9). The mean EV with four stations removed is only slightly larger than that without removing data, even though the mean fractional decrease is larger. Removing six stations usually produces larger initial EV than found with no stations removed. At 1500 and 1600 CST, when the STL 002 data were not included in the interpolation, the reduction of the EV is slightly greater, but not enough to reduce the EV relative to the basic case.

The nighttime winter cases showed a more variable error reduction, averaging about 28 percent regardless of the number of observations deleted. The analyses seem to produce a 22 to 28 percent decrease in EV regardless of the concentration or number of stations removed. The reduction is generally less (nearer 22 percent) during the daytime. The resultant error appears to be a result of the initial error.

ACCURACY ESTIMATES

In the summer case, the average CO observed concentration was 0.6 ppm and ranged from 0.1 ppm to 2.0 ppm. The RMS difference between the observed and predicted concentrations at non-network stations was $\pm$ 0.6 ppm. When two or four stations were deleted, the RMS difference did not change; but when six stations were deleted, the RMS difference decreased slightly to $\pm$ 0.4 ppm. The decrease was primarily due to the deletion of EPA 105 and STL 002 which had observed concentrations inconsistent with the local emissions. When these stations were included, their observations markedly influenced the initial conditions produced by the Barnes algorithm and the resultant OVAM analysis over a broad area. When these stations were deleted, the concentrations increased near the center of the city and decreased to the south relative to the case when these stations were included, in response to the local emission--and, thus, increased the accuracy at non-network stations. The inconsistencies were likely due at least in part to differences in the nature of the data--point observations and area-averaged sources--and to location

TABLE 4. NON-DIMENSIONAL ERROR VARIANCE OF ANALYSES

		Stations Removed											
		None			Two			Four			Six		
Date	Hour	Barnes	OVAM	% DECR	Barnes	OVAM	% DECR	Barnes	OVAM	% DECR	Barnes	OVAM	% DECR
	11	197	158	20	236	173	27	181	149	18	295	195	34
	12	202	174	14	234	196	16	188	167	11	248	195	21
Aug	13	260	216	16	283	236	17	269	229	15	284	231	19
14	14	331	259	22	355	281	21	328	265	19	354	267	25
	15	487	357	25	543	394	27	523	393	25	419	314	25
	16	369	271	27	388	279	28	390	295	24	309	247	20
	17	132	97	26	119	96	19	112	95	14	171	118	31
	18	65	53	19				63	52	16	67	51	24
				21.1			22.1			17.8			24.9
	18	.533	.378	29							1.36	.998	27
Feb	19	.389	.275	29							.634	.469	26
18	20	1.40	1.20	14							4.31	3.32	23
	21	1.65	1.15	30							3.92	2.56	35
				25.5									27.8
	18	.517	.368	29							1.10	.762	31
	19	1.69	1.23	27							2.64	2.01	24
Feb	20												
26	21	2.25	1.78	21							3.11	2.52	19
	22	8.65	5.69	34							7.53	4.70	38
	23	1.59	1.15	28							4.01	2.73	32
				27.8									28.8
	00	3.01	1.54	49							4.06	2.76	32
	01	1.49	1.26	16							3.48	2.47	29
	2	0.827	.615	26							1.68	1.38	18
	3	0.395	.320	19							.77	0.61	21
Feb	4	0.115	.098	15							1.53	1.01	35
27	5	11.11	6.83	38							11.72	5.69	51
	6	.842	.663	22							71.69	58.77	18
	7	1.68	1.16	31							1.57	1.18	25
	8	5.31	2.64	50							3.73	2.70	28
				29.5									28.6
				26.0									27.3

BEGIN FIRST LINE OF TEXT HERE
TYPING GUIDE SHEET
CENTER OF PAGE
TOP OF IMAGE AREA
DROPPED HEAD: BEGIN SECTIONS HERE
6-1/2"
9-1/8"
BEGIN LAST LINE OF TEXT
3/8"
BOTTOM OF IMAGE AREA: OUTSIDE DIMENSION FOR TABLES AND ILLUSTRATIONS
PAGE NUMBER
EPA-287 (Cin.) (4-76)

differences between the observation and the grid point--grid points were up to 0.7 km from the observations.

In the winter, the average observed CO concentration was 5.3 ppm and ranged from 1.0 to 15 ppm. The RMS difference was $\pm$ 4.2 ppm. When six stations were deleted, the RMS difference increased to $\pm$ 6.5 ppm. During the early morning hours of 27 February 1976, the concentrations that would be produced by the emissions were considerably smaller than the actual observations (by an order of magnitude). The emissions decreased due to the inactivity in the city. The CO concentrations remained large and were apparently left over from the rush hour emissions. The OVAM analysis was controlled by the initial conditions and the dynamic effect of the wind, the influence of the former dominating. At night when emissions are small, the initial conditions must very nearly represent the actual field. This can be accomplished by utilizing the previous hours analysis updated with existing observations as the initial field, but this procedure must begin during periods of large emissions.

BEGIN FIRST LINE OF TEXT HERE
TYPING GUIDE SHEET
CENTER OF PAGE
TOP OF IMAGE AREA
DROPPED HEAD; BEGIN SECTIONS HERE

DISCUSSION OF RESULTS

MAJOR FINDINGS

The OVAM was adapted for field data and applied to CO concentrations obtained from the OSN. Several cases representing a variety of conditions were examined with the objective of assessing the model sensitivity to input parameters, the response characteristics of the analyses, the reduction of error variance, the effects of missing data, and the overall effectiveness of the model.

The OVAM analysis was particularly sensitive to the ratio of weights for the observations and constraint equation but was insensitive to the radius of influence of the observation. The grid spacing was a practical lower limit to the radius of influence since it was half the resolvable spatial scale. However, CO concentrations are highly variable on a small scale, suggesting a small radius of influence should be utilized. OVAM analyses became smoother and less sensitive to emissions as the depth of the volume, Z, increased. Increasing Z diluted the emissions over a large volume. A practical upper limit to Z might be the atmospheric mixing height. The choice of Z was also important because point sources that fail to rise above Z were treated as area sources.

Results of the application of the OVAM to the August 12, 1975 case (daytime) showed a strong dependence upon the spatial distribution of sources and winds. Upwind of the stronger area sources, the concentrations tend to decrease; downwind, they increase. Large percentage changes between the initial guess and the OVAM analysis were found in the vicinity of principal sources. Since concentrations were on the order of 0.5 ppm, which is rear the practical limit of observations for CO, the percent changes are relatively meaningless, except to help identify the on-going processes.

For the 27 February 1976 case (nighttime), the CO emissions decreased by an order of magnitude, whereas the concentrations remained high. The OVAM produced analysis that did not differ greatly from the initial guess. The principal adjustments of the analysis were due to boundary conditions and winds because the magnitude of the source emissions were inconsistent with the magnitude of the observed concentrations.

The response of the analyses to deleting two, four, or six observations from the OSN produced inconclusive and, at times, conflicting results. The error variance decreased by 20 to 30 percent of its initial value regardless of the number of stations deleted. However, large percentage changes of concentration occurred, depending upon the location of deleted data. In most daytime cases, the largest changes occurred when observations upwind or

BEGIN LAST LINE OF TEXT
BOTTOM OF IMAGE AREA, OUTSIDE DIMENSION FOR TABLES AND ILLUSTRATIONS
3/8"

EPA-287 (Cin.)
(4-76)

BEGIN FIRST LINE OF TEXT HERE
TYPING GUIDE SHEET
CENTER OF PAGE
TOP OF IMAGE AREA
DROPPED HEAD: BEGIN SECTIONS HERE

downwind of principal source areas were deleted, and when the deleted observations were not near other observations which were near principal sources. Large changes were also found when changes in background concentration occurred. In all cases, the concentration changes were primarily controlled by changes in the initial guess resulting from the deleted observations.

When stations, which were in regions where the emissions were small or non-existent (the outlying regions of the city) and which were not near stations influenced by large sources, were deleted, the impact was significant in those regions, but relatively insignificant in the large emission regions. The impact at the deleted stations in the outlying regions was primarily due to the interpolated initial value being different from the observation, suggesting that, if initial conditions can be treated properly in the outlying regions, some of the stations in this region would not be required as a CO monitoring station. Thirteen of the nineteen OSN stations were in such regions. Possibly as many as half of these need not monitor CO, though they all must monitor the wind. However, further investigation is required on initialization methodology before conclusive statements can be made. The sample is too small and the relationship of the 1 km square sources to the point measurements is not well-defined. The cause-effect relationships are tied to the density of the stations, the initial guess of the concentrations at those stations and, of course, upon the meteorological conditions.

In several instances the OVAM did not predict concentrations in agreement with observed concentrations at the non-network stations. The discrepancies arose because 1) the CO concentrations tend to be source-oriented, and sources are smoothed to a 1 km square area by the inventory (this problem affects all CO data) whereas the observations are point observations not necessarily representative of an area; and 2) the OVAM values used for comparison were at grid points up to .7 km from the observation. The OVAM developed plumes with strong gradients perpendicular to the wind downwind of principal sources. Those plumes may be slightly offset from the grid point while actually affecting the station.

The impact of boundary conditions upon the analyses was not significant, but the boundary conditions currently used were somewhat arbitrary. Further study is needed to determine if a set of boundary conditions can be established which have a better foundation.

LIMITATIONS AND FURTHER RESEARCH

The OVAM analysis was limited by the inconsistency in the mixture of data available for application in the model. Time-averaged, point observations and area-averaged emissions were two of the primary data inputs. Time-averaged CO concentrations at a point are poor representations of an area-averaged concentration, especially in urban areas. The location of a sampler relative to a nearby source is extremely critical for determining the CO concentration. The area-averaged emission smoothes the local variability of CO sources. Thus, the local source/receptor relationship so often found with CO measurements is not necessarily identifiable using area averaged data. The inconsistency went both ways: sometimes the concentrations were higher than

BEGIN LAST LINE OF TEXT
BOTTOM OF IMAGE AREA OUTSIDE DIMENSION FOR TABLES AND ILLUSTRATIONS
3/8"

EPA-287 (Cin.)
(4-76)

BEGIN FIRST LINE OF TEXT HERE
TYPING GUIDE SHEET
CENTER OF PAGE
TOP OF IMAGE AREA
DROPPED HEAD, BEGIN SECTIONS HERE

that developed by the emissions inventory, and other times they were lower. This is a shortcoming faced by modellers and analysts everyday.

Sophisticated analysis algorithms such as the OVAM will produce results in accordance to the input data and model parameters. Consistent analyses can usually be acquired only if consistent input data are available. However, there is a possibility to obtain a consistent analyses utilizing the OVAM through manipulation of certain model parameters, namely the weights. In its present form, the model places total emphasis on the observation at the location of the observations. Two and one-half kilometers from that point, the entire emphasis is placed on the constraint equation. The present concensus is that a certain amount of emphasis, which can be achieved by manipulation of the weights, should be placed on the constraint equation at the location where the observations are found. This procedure will force the observation and the emissions to become mutually consistent. Proper selection of the weights which would produce a more consistent analysis must be left to research. Such research is essential for proper application of the OVAM.

The OVAM relied upon the initial conditions generated by the Barnes analysis to determine the concentration in data-sparce areas. The CO concentration is uncorrelated at distances as small as 1 km; yet the Barnes analysis extends the radius of influence of an observation considerably farther than 1 km. For example, the OVAM analysis for 1300 and 1400 CST 12 August, when station STL 002 did not report, showed large concentrations in a narrow plume over and downwind from STL 002. At 1500 and 1600 CST, when STL 002 reported a very large CO concentration, the plume extended over almost half the southern region of the grid because the Barnes analysis produced an initial field in which the observation at STL 002 dominated the southern area. The OVAM results were not in agreement with the observations at many of the other OSN stations as well as non-network stations. When STL 002 was deleted at 1500 and 1600 CST and a new set of initial conditions were developed, the OVAM results were in better agreement with both the OSN and the non-network observations at those hours and with the analyses at 1300 and 1400 CST. Though part of the problem in this case resulted from inconsistencies in the data mixture, the differences in the area influenced by the large sources around STL 002 with and without the observation at STL 002 was completely dependent on the initial conditions generated by the Barnes method.

Better initialization procedures are highly desirable. Other interpolation procedures would undoubtedly produce similar results as those produced by the Barnes method. Research into initialization procedures is necessary to obtain a high quality analysis from the OVAM. One procedure with a high potential for success is the use of the observations at the specified grid points, filling in the remaining grid points with a background value defined to be the network average or minimum value. In this manner, the influence of the observation is initially confined to a specific grid point in accordance with the notion that CO becomes rapidly uncorrelated in space. Initial conditions specified in this manner would allow the OVAM to develop completely the distribution rather than altering some initial distribution.

The problems with data mixture and initialization are the most dominant problems confronted in utilization of the OVAM. They can interact, producing

BEGIN LAST LINE OF TEXT HERE
BOTTOM OF IMAGE AREA, OUTSIDE DIMENSION FOR TABLES AND ILLUSTRATIONS
3/8"

PAGE NUMBER
EPA-287 (Cin.) (4-76)

BEGIN FIRST LINE OF TEXT HERE
TYPING GUIDE SHEET
CENTER OF PAGE
TOP OF IMAGE AREA
DROPPED HEAD: BEGIN SECTIONS HERE

analyses that are inconsistent in time, and, at a given hour, are in poor agreement with the OSN and non-network observations. It is essential that research continues to solve these problem areas. Other problem areas involving boundary conditions and the choice of the top of the model should also be investigated.

UTILIZATION OF THE OSM TECHNIQUE

Except for some improvements needed for the OVAM, the essential ingredients for the OSN technique had been developed and tested, and the test results have been shown to be reasonable. The OSN technique provides an objective method to develop a sampling network for air pollution and meteorological parameters that will yield a representative distribution of the air pollution and meteorological parameters within the domain of the network. Though the technique has been used to develop an entire network, probably the greatest utilization of the technique may be in improving an existing network in a given urban area. Most urban areas already have a sampling network and would not want to undertake the economic burden to establish a new network.

The site selection algorithm of the OSN technique can be altered so as to maintain certain sites as part of the improved network (the stations in the existing network). The algorithm would then establish the minimum number of stations and their locations needed to be added to the existing network in order to determine a reasonable analysis of the wind field. The OVAM, the model used to obtain the air pollution distribution is independent of the network design. However, since the wind field is an input to the OVAM, an accurate description of the wind field is necessary. Given the emissions inventory, then the air pollution distribution can be determined.

The procedure of updating existing networks has not been tested nor has the site selection algorithm been adjusted to accommodate the procedure. The existing data for St. Louis can be utilized to test of the OSN technique for updating networks. A nine-station sampling network presently exists in St. Louis. RAPS and RTI stations can be used as a part of the updated network. Case studies would be identical to those utilized for the OSN developed for St. Louis, simplifying the analysis.

BEGIN LAST LINE OF TEXT
BOTTOM OF IMAGE AREA; OUTSIDE DIMENSION FOR TABLES AND ILLUSTRATIONS
3/8"

EPA-287 (Cin.)
(4-76)

BEGIN FIRST LINE OF TEXT HERE
TYPING GUIDE SHEET
CENTER OF PAGE
TOP OF IMAGE AREA
DROPPED HEAD; BEGIN SECTIONS HERE
6-1/2"
9 1/8"
BEGIN LAST LINE OF TEXT
BOTTOM OF IMAGE AREA OUTSIDE DIMENSION FOR TABLES AND ILLUSTRATIONS
3/8"
PAGE NUMBER
EPA-28T (Cin.)
(4-76)

Weighted interpolation analyses fall short by smoothing the analysis in a highly variable scalar and by underestimating large values and overestimating small ones. Maxima and minima occur only near maxima and minima in the input field. Barnes improves the initial analysis by interpolating the differences of the observed and interpolated values $\delta_{i,n} = \hat{\phi}_{i,n} - \phi_{i,n}$ over a small area near the observation. By adding the two fields, the new estimate of $\hat{\phi}$ at the observation time and place should be improved. For the second interpolation, Barnes shows that using W^{γ} as the weight function for the $\delta_{i,n}$ analysis is equivalent to using an iterative error reduction. In practice, γ, exceeds 2 but is usually less than 5.

BEGIN FIRST LINE OF TEXT HERE
TYPING GUIDE SHEET
CENTER OF PAGE
TOP OF IMAGE AREA
DROPPED HEAD: BEGIN SECTIONS HERE

REFERENCES

Barnes, S. L. 1964. "A Technique for Maximizing Details in Numerical Weather Map Analysis:, J. Appl. Meteor., 3, 396-409.

Chaney, L. W. 1979. "Microscale Variations in Ambient Concentrations of Pollutants in St. Louis Air", EPA-600/2-79-183, US EPA Environmental Sciences Research Laboratory, Research Triangle Park, NC 27711.

Cressman, G. P. 1959. "An Operational Objective Analysis Systems", Mon. Wea. Rev., 87, 367-374.

Endlich, R. M. and R. L. Mancuso. 1968. "Objective Analysis of Environmental Conditions Associated with Severe Thunderstorms and Tornadoes", Mon. Wea. Rev., 96, 342-350.

Lanczos, C. 1970. The Variational Principles of Mechanics, Fourth Edition, University of Toronto Press, Toronto.

Ludwig, F. L. and J. H. S. Kealoha. 1975. "Selecting Sites for Carbon Monoxide Monitoring", EPA-450/3-75-007, US EPA, Research Triangle Park, NC 27711.

Novak, J. H. and D. B. Turner. 1976. "An Efficient Gaussian Plume Multiple Source Air Quality Algorithm", J. Air Poll. Control Assoc., 26, 570-575.

Ott, W. R. and R. Eliassen. 1973. "A Survey Technique for Determining the Representativeness of Urban Air Monitoring Stations with Respect to Carbon Monoxide", J. Air Poll. Control Assoc., 23, 685.

Ott, W. R. 1977. "Development of Criteria for Siting Air Monitoring Stations", J. Air Poll. Control Assoc., 27, 543.

Sasaki, Y. 1958. "An Objective Analysis Based on the Variational Method", J. Meteor. Soc., Japan, 36, 77-88.

_____. 1970a. "Some Basic Formalisms in Numerical Variational Analysis", Mon. Wea. Rev., 98, 875-883.

_____. 1970b. "Numerical Variational Analysis Formulated Under the Constraints as Determined by Long-Wave Equations and a Low-Pass Filter", Mon. Wea. Rev., 98, 884-898.

_____. 1970c. "Numerical Variational Analysis with Weak Constraint and Application to Surface Analysis of Severe Storm Gusts", Mon. Wea. Rev., 98, 899-910

BEGIN LAST LINE OF TEXT HERE
3/8"
BOTTOM OF IMAGE AREA, OUTSIDE DIMENSION FOR TABLES AND ILLUSTRATIONS

EPA-287 (Cin.) (4-76)

BEGIN FIRST LINE OF TEXT HERE
TYPING GUIDE SHEET
CENTER OF PAGE
TOP OF IMAGE AREA
DROPPED HEAD BEGIN SECTIONS HERE

_____, and J. M. Lewis. 1970. "Numerical Variational Objective Analysis of the Planetary Boundary Layer in Conjunction with Squall Line Formation", J. Meteor. Soc. of Japan, 48, 381-398.

Stephens, J. J. 1970. "Variational Initialization with the Balance Equation", J. Appl. Meteor., 9, 732-739.

Thompson, P. D. 1961. Numerical Weather Analysis and Prediction, The MacMillan Company, New York.

Vukovich, F. M., W. D. Bach, Jr. and C. A. Clayton. 1978. "Optimum Meteorological and Air Pollution Sampling Network Selection in Cities, Vol. I: Theory and Design for St. Louis", EPA-600/4-78-030, US EPA Environmental Monitoring Systems Laboratory, Las Vegas, NV 89114

_____, and C. A. Clayton. 1979. "Optimum Meteorological and Air Pollution Sampling Network in Cities, Vol. II: Evaluation of Wind Field Predictions for St. Louis", EPA-600/4-79-069, US EPA Environmental Monitoring Systems Laboratory, Las Vegas, NV 89114

Wilkins, E. M. 1971. "Variational Principle Applied to Numerical Objective Analysis of Urban Air Pollution Distribution", J. Appl. Meteor., 10, 974-981.

_____. 1972. "Variationally Optimized Numerical Analysis Equations for Urban Air Pollution Monitoring Networks", J. Appl. Meteor., 11, 1334-1341.

BEGIN LAST LINE OF TEXT
BOTTOM OF IMAGE AREA OUTSIDE DIMENSION FOR TABLES AND ILLUSTRATIONS
1/2"

PAGE NUMBER
EPA-282 (Cont.)
(4-78)

BEGIN FIRST LINE OF TEXT HERE
TYPING GUIDE SHEET
CENTER OF PAGE
TOP OF IMAGE AREA
DROPPED HEAD. BEGIN SECTIONS HERE

APPENDIX A
OBJECTIVE ANALYSIS TECHNIQUE

Barnes used a weighted space-time interpolative procedure to ascertain winds, temperature, and moisture in the vicinity of a moving thunderstorm. The procedure is fairly simple and straightforward. If $\hat{\phi}_o = \phi(x_o, y_o, t_o)$ is the scalar variable to be interpolated from a set of observations $\hat{\phi}_{i,n} = \phi(x_i, y_i, t_n)$, then a weighted interpolation analysis technique is written:

$$\hat{\phi}_o = \frac{\sum_i \sum_n w(r_i, r_o, t_n, t_o) \cdot \phi_{i,n}}{\sum_i \sum_n w(r_i, r_o, t_n, t_o)}$$

where $r^2 = x^2 + y^2$.

Barnes chooses w, the weight function, as

$$w(r_i, r_o, t_n, t_o) = a \exp \left\{ - R^2/4k^{*2} - T^2/4v^2 \right\} / 8\pi^{3/2} k^* v$$

where

$$R^2 = (x_i - x_o)^2 + (y_i - y_o)^2$$

$$T = t_n - t_o$$

$$4k^{*2} = 4k^* (1 + B \cos^2 \psi)$$

$B = V_i/V^*$ for $V^* > 0$, $= 0$ otherwise,
ψ = the angle between the position vector from r_o to r_i and the wind velocity vector $\vec{V}_i$

$$V_i = |\vec{V}_i|$$

and V^* = a characteristic speed of the system moving past the observing locations.

The parameters k and v are chosen according to the data density and the scale of motions represented by the analyses. The term a represents the confidence in the data. If the data is suspect, then a is small (<1); whereas with total confidence in the data, a = 1.0.

BEGIN LAST LINE OF TEXT HERE
BOTTOM OF IMAGE AREA OUTSIDE DIMENSION FOR TABLES AND ILLUSTRATIONS
PAGE NUMBER
EPA-287 (Rev.) (4-76)